NASA Contractor Report 187490

NASA-CR-187490
19910015854

CONTROL AND STRUCTURAL OPTIMIZATION FOR MANEUVERING LARGE SPACECRAFT

Final Report

H. M. Chun, J. D. Turner, and C. C. Yu

MCDONNELL DOUGLAS SPACE SYSTEMS COMPANY
Huntington Beach, California
and
PHOTON RESEARCH ASSOCIATES, INC.
Cambridge, Massachusetts

Contract NAS1-18763
October 1990

National Aeronautics and Space Administration

Langley Research Center
Hampton, Virginia 23665-5225

NASA
National Aeronautics and Space Administration

Report Documentation Page

1. Report No.	2. Government Accession No.	3. Recipient's Catalog No.
NASA CR-187490		

4. Title and Subtitle
Control and Structural Optimization for Maneuvering Large Spacecraft

5. Report Date
October 1990

6. Performing Organization Code

7. Author(s)
H. M. Chun, J. D. Turner, and C. C. Yu

8. Performing Organization Report No.

10. Work Unit No.
590-14-51-01

9. Performing Organization Name and Address

McDonnell Douglas
Space Systems Co.
5301 Bolsa Ave.
Huntington Beach, CA 92647

Photon Research Assoc.
Cambridge Research Div.
1033 Massachusetts Ave.
Cambridge, MA 02138

11. Contract or Grant No.
NAS1-18763

13. Type of Report and Period Covered
Contractor Report

12. Sponsoring Agency Name and Address
National Aeronautics and Space Administration
Langley Research Center
Hampton, VA 23665-5225

14. Sponsoring Agency Code

15. Supplementary Notes
Langley Technical Monitor: Suresh Joshi
Final Report

16. Abstract

This report presents the results of an advanced control design and discusses the requirements for automating both the structures and controls design efforts. The advanced control application addresses a general three dimensional slewing problem, and is applied to a large geostationary platform. The platform consists of two flexible antennas attached to the ends of a flexible truss. The control strategy involves an open-loop rigid body control profile which is derived from a nonlinear optimal control problem and provides the main control effort. A perturbation feedback control reduces the response due to flexibility of the structure. Results are shown which demonstrate the usefulness of the approach. The test cases involve slew maneuvers with periods close to the period of the first mode and two sets of control actuators are considered.

Software development issues are considered for developing an integrated structures and control design environment. This development is driven by the recognized need to coordinate both the structure and control design efforts to minimize mission threatening control/structure interactions.

17. Key Words (Suggested by Author(s))	18. Distribution Statement
slew maneuvers, optimal control, control/structure interaction, control/structure optimization, integrated design, perturbation feedback	Unclassified - Unlimited Subject Category 18

19. Security Classif. (of this report)	20. Security Classif. (of this page)	21. No. of pages	22. Price
Unclassified	Unclassified	80	

NASA FORM 1626 OCT 86

N91-25168#

NASA Contractor Report 187490

CONTROL AND STRUCTURAL OPTIMIZATION FOR MANEUVERING LARGE SPACECRAFT

Final Report

H. M. Chun, J. D. Turner, and C. C. Yu

MCDONNELL DOUGLAS SPACE SYSTEMS COMPANY
Huntington Beach, California
and
PHOTON RESEARCH ASSOCIATES, INC.
Cambridge, Massachusetts

Contract NAS1-18763
October 1990

National Aeronautics and
Space Administration

Langley Research Center
Hampton, Virginia 23665-5225

TABLE OF CONTENTS

INTRODUCTION

The design of future large space structures will require the development of advanced control systems in order to meet stringent pointing requirements. There are two types of operational environments that are of interest. First, earth pointing applications from geostationary orbits. These applications are characterized by vibration and shape control problems which must operate within a persistent disturbance environment. Second, maneuvering or slewing applications where the vehicle is transferred from an initial pointing direction to a final desired pointing direction in finite time. A key issue for maneuver problems is that the desired rigid body pointing direction is achieved while suppressing any maneuver induced structural response. The technical solutions for these applications are fundamentally different. For example, the vibration and shape control applications represent infinite time or steady state problems, where the major concern is system stability. The stability questions arise because the control system is continuously generating command inputs in an effort to suppress the structural response induced by the persistent disturbance sources. As a result, if the mathematical model used for designing the control has errors, the potential exists for exciting a resonance response due to control spillover effects. Slewing control problems, on the other hand, represent finite-time control problems because the maneuvers are usually designed to be accomplished within a specified period of time. Even though the maneuver loads tend to be large compared with typical on-board or environmental disturbances, their finite time duration tends to minimize the potential for exciting resonance responses due to modeling errors.

The report presents an advanced control design problem and discusses the requirements for automating both the structures and controls design efforts. First, a general three dimensional slewing technique is developed and applied to a large geostationary platform. This system presents significant technical challenges because of two large flexible antennas which are attached to a flexible truss structure. The control problem formulation treats the full nonlinear coupled rigid and flexible body control problem. Second, the software development issues are considered for developing an integrated structures and control design environment. This development is driven by the recognized need to coordinate both the structures and control design efforts to minimize mission threatening control/structure interactions.

SLEW CONTROL METHODOLOGY

Control Strategy

The structure used in this study is the Earth Pointing Satellite (EPS) shown in Fig. 1. The control methodology for the Class III slew control of the EPS model follows the approach of Chun, Turner, and Juang, 1987. The approach consists of an optimal open-loop maneuver designed for a rigid model of the EPS structure, and a closed-loop perturbation feedback designed for a reduced order flexible model. The rigid body controls are applied to the flexible plant. The difference between the nominal rigid body response and the actual flexible response is then fed to the perturbation feedback controller to generate control corrections that cause the flexible structure to follow the rigid body response as closely as possible. Both the open-loop and the closed-loop controllers are designed using frequency-shaping techniques that impose a two-pole roll-off in the frequency domain of the control effort.

While the results of Chun, Turner, and Juang, 1987 were obtained with a fair separation of control and structure bandwidths, the current study involves maneuvers where the bandwidths are much closer. The current work also introduces a disturbance accommodating feedforward term into the control strategy that compensates for the excitation of the elastic degrees of freedom due to the nominal controls.

Model Development

The structure is developed by the CSI Analytical Design Methods (ADM) team at NASA LaRC. The structural design is a derivative of a geostationary platform designed in support of Earth Observation Sciences (EOS).

The total mass of the vehicle is 1028 kg. It consists of 548 kg of structural mass, 329.63 kg of nonstructural mass on the antennas, and 150 kg of actuator mass. The truss in Fig. 1 is about 25 m long while the two antennas are 15 m and 7.5 m in diameter. There are supports for each of the antennas. A more detailed description of the structure and material properties are presented in the following paragraphs.

The truss is a 3 meter total cross section structure. The truss consists of 51 mm diameter x 1.59 mm wall thickness graphite tubes. The modules of elasticity and mass density for the tubes are 275.9E+09 N/m^2 and 3250 kg/m^3 respectively. There are total of 135 beam elements that form the truss.

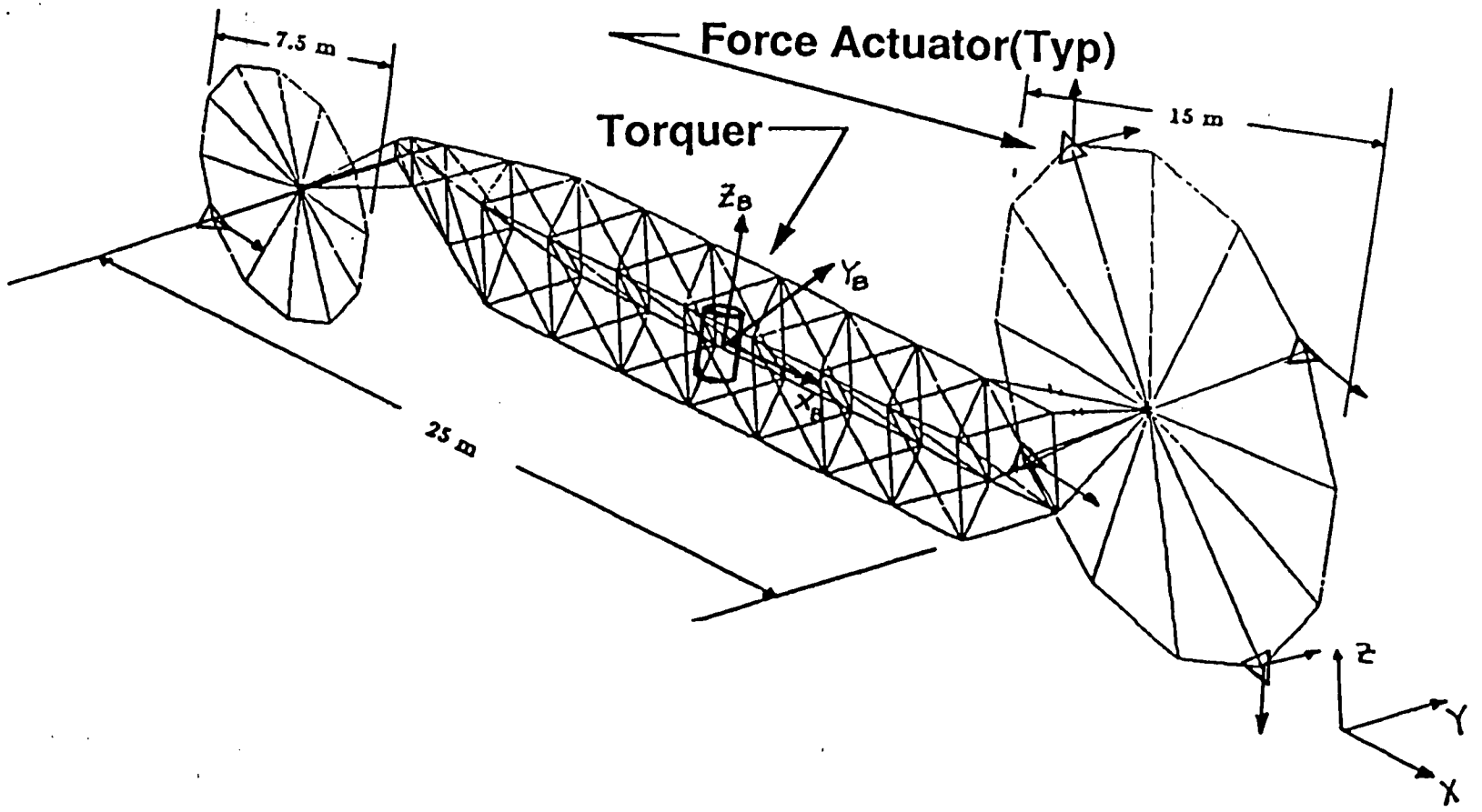

Figure 1. EPS Structural Model

Both the 15 m and 7.5 m antennas have 12 ribs which radiate outward from the center. The ends of the ribs are connected by hoop elements. Graphite tube diameters and thicknesses for the antennas are the same as those used for the truss elements. The support of each antenna consists of four beam elements that offset the antenna from the main truss (see Fig. 1).

Torquers are located at the CG of the vehicle, acting about all three axes to provide the slewing motion. The support for the actuators is made of the same element sizes and mechanical properties as the truss elements.

The first 20 undamped vibration frequencies and their corresponding modal descriptions are:

Mode No.	Frequency in Hz	Description
1-6	0.0	Rigid Body
7	0.2422	Torsion of 15 m Antenna
8	0.4056	z-rotation 15 m Antenna
9	0.5652	x-rotation 15 m Antenna
10	0.6562	Torsion 7.5m Antenna
11	0.8882	15 m Antenna mode
12	0.8882	15 m Antenna mode
13	1.4377	z-rotation 7.5 m Antenna
14	1.5360	x-rotation 7.5 m Antenna
15	1.7762	15 m Antenna mode
16	1.7762	15 m Antenna mode
17	3.0258	15 m Antenna mode
18	3.0258	15 m Antenna mode
19	3.1532	15 m Antenna mode
20	3.1532	15 m Antenna mode

It should be noted that the first 20 undamped elastic modes are all antenna modes. The first truss vibration mode occurs at a relatively high frequency, about 7.0 Hz, which is the 50th elastic mode. The NASTRAN EPS model has been generated by Joe Walz at NASA LaRC. It consists of a total of 95 nodes and 223 elements. The truss and the two antennas are treated in the model as a single body. The finite element data used in DISCOS includes the modal frequencies of the first 45 elastic modes, the translation and rotation modal shapes for all 95 nodes, and lumped masses at each node point. Modal damping of 0.5% is added for each mode. Inertial integrals are generated by DISCOS from mode shape and lumped mass data to account for the coupling between rigid and flexible body dynamics.

Actuator Placement

It is well known that force actuation at various locations of a large space structure can provide significant vibration suppression of the structure. A preliminary force actuator analysis is performed to determine the force actuator locations. The objective of the actuator placement task is to find a set of feasible, but not necessarily optimal, actuator locations so that force actuators can be used for performance enhancement.

Potential force actuators can be lightweight variable cold gas thrusters, and potential torquers can be CMG or reaction wheels. The force actuators and torquers are modeled as external forces and torques; no force actuator, CMG or reaction wheel dynamics are modeled. The commanded forces and torques are frequency-shaped so that there is very little energy at the high frequency end of the control spectrum. Furthermore, the force actuators and torquers are not output limited.

For this study, two actuator placement algorithms have been examined - an H_2 optimization algorithm (Fanson, Blackwood, and Chu, 1989) and a degree of controllability algorithm (Longman and Alfriend, 1990, and Viswanathan, Longman, and Likins, 1984). The H_2 optimization algorithm was developed by Jim Fanson at the Jet Propulsion Laboratory to preselect the actuator locations on a truss structure. This algorithm has the advantage that it is theoretically simple and numerical computation can be readily performed by standard control design tools such as Ctrl-C. Its disadvantage is that the algorithm lacks strong theoretical support. The H_2 formulation assumes that the external disturbances are white or colored noise.

Based on engineering intuition, one would expect elastic deformations at extremal locations of a large spacecraft to be large. Hence, the outer rims of the EOS antennas are expected to provide better actuator locations than locations on the truss. The suitability of the locations at the outer rims of the antennas has been confirmed by both simulation and actuator placement studies. A detailed description of the algorithm is presented in the following paragraphs.

The cost function is selected to be a linear combination of the total energy of the position vector y at specified nodes and the control vector u, subject to disturbances generated by the torquers located at the CG. It is assumed that the disturbance is a low bandwidth colored noise. This formulation provides a well-posed H_2 optimization problem where an analytical closed-form solution exists. Full state information is assumed in the present analysis.

In mathematical terms, the H_2 optimization problem for actuator placement is defined as

$$\beta = \min_{u_k \in L_2(0,\infty)} \|z\|_2^2 \tag{1}$$

where

$$z = [\gamma y \;\; u]^T; \quad \gamma > 0$$

γ is a positive constant weighting factor, $y(t)$ and $u(t)$ are the output and control of the system, respectively, and $\|\bullet\|$ represents the Euclidean norm.

For simplicity, only the modal state equations are considered. The corresponding state-space equations are

$$\dot{x} = Ax + Bu + b_w w \tag{2}$$

and

$$z = \begin{bmatrix} \gamma C \\ 0 \end{bmatrix} x + \begin{bmatrix} 0 \\ I \end{bmatrix} u \tag{3}$$

The unique optimal control is expressed as

$$u = Fx \tag{4}$$

where

$$F = -B^T X$$

and X is the positive definite solution to the following Riccati equation:

$$A^T X + XA - XBB^T X + \gamma^2 C^T C = 0$$

The minimal cost can be expressed as

$$\beta = \left(b_w^T X b_w\right)^{1/2} \tag{5}$$

The total energy in y and u can be computed by using

$$\|y\|_2 = \left[\text{trace}\left(CW_cC^T\right)\right]^{1/2} \tag{6}$$

$$\|u\|_2 = \left[\text{trace}\left(FW_cF^T\right)\right]^{1/2} \tag{7}$$

where W_C is the solution of the following Lyapunov equation:

$$(A + BF)\, W_C + W_C\, (A + BF)^T + BB^T = 0$$

The total energy in each control input, u_i, of the optimal control u is computed as follows:

$$\|u_i\|_2 = \left(b_i^T W_o b_i\right)^{1/2} \tag{8}$$

where b_i is the i-th column of the control influence matrix B, and W_O satisfies the following Lyapunov equation:

$$(A + BF)^T\, W_O + W_O\, (A + BF) + F^T F = 0$$

In this preliminary actuator placement analysis, the disturbance input is provided by the torquers located at the CG (node 95) of the vehicle. The candidate force actuator locations are arbitrarily selected to be nodes 69, 66, 63, 60, 52, 95, 94, 88, and 78 along all 3 axes, while the output of the system is chosen to be at nodes 69, 66 and 95 (CG of the vehicle) along all 3 axes (see Fig. 2). Equation (8) is used to evaluate actuator effectiveness. The five top ranking actuator locations based on a modal energy consideration are:

Rank	Actuator	Location
1	Node 69	x
2	Node 66	x
3	Node 63	x
4	Node 60	x
5	Node 88	x

These five actuator locations are input into DISCOS for plant linearization as part of the perturbation feedback design. The linearized system dynamics matrix and the control influence matrix are used to compute feedback gains using LQR theory. However, the resulting closed-loop dynamics matrix is found to be unstable because the selected actuator locations do not provide the controllability required. A controllable system is obtained after switching two of these five actuators to be along the y and z directions, leading to:

Actuator	Direction
Node 69	x
Node 63	x
Node 66	y
Node 60	z
Node 88	x

Theoretically, the five force actuators, together with the torquers at the CG provide sufficient controllability. However, simulations indicate that the elastic displacements at opposite ends of the antenna rims tend to be opposite to each other in sign, with approximately the same magnitude. This observation suggests that the actuators be placed in pairs at opposite sides on the antenna rim where peak displacements are experienced. Accordingly, two force actuators are added to the above set of five actuators at node 66 in the z direction and node 60 in the y direction. No attempt has been made to add an additional actuator opposite to node 88 x because the magnitude of the elastic deformation at the 7.5 m antenna is about a factor of 5 smaller than that of the 15 m antenna. The final set of actuators selected is listed below:

Actuator	Direction
Node 69	x
Node 63	x
Node 66	y,z
Node 60	y,z
Node 88	x

By including these force actuators, satisfactory performance is achieved.

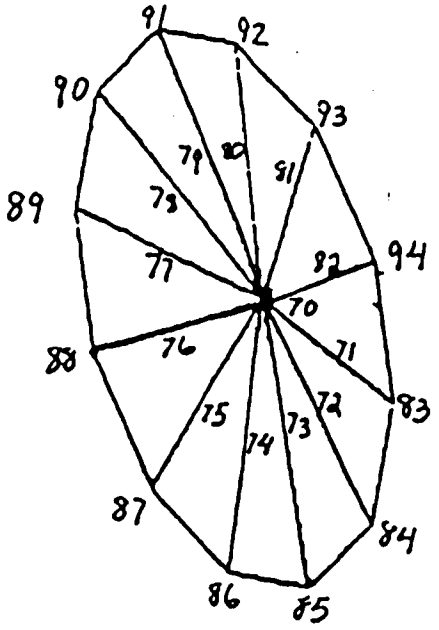

7.5 M Antenna

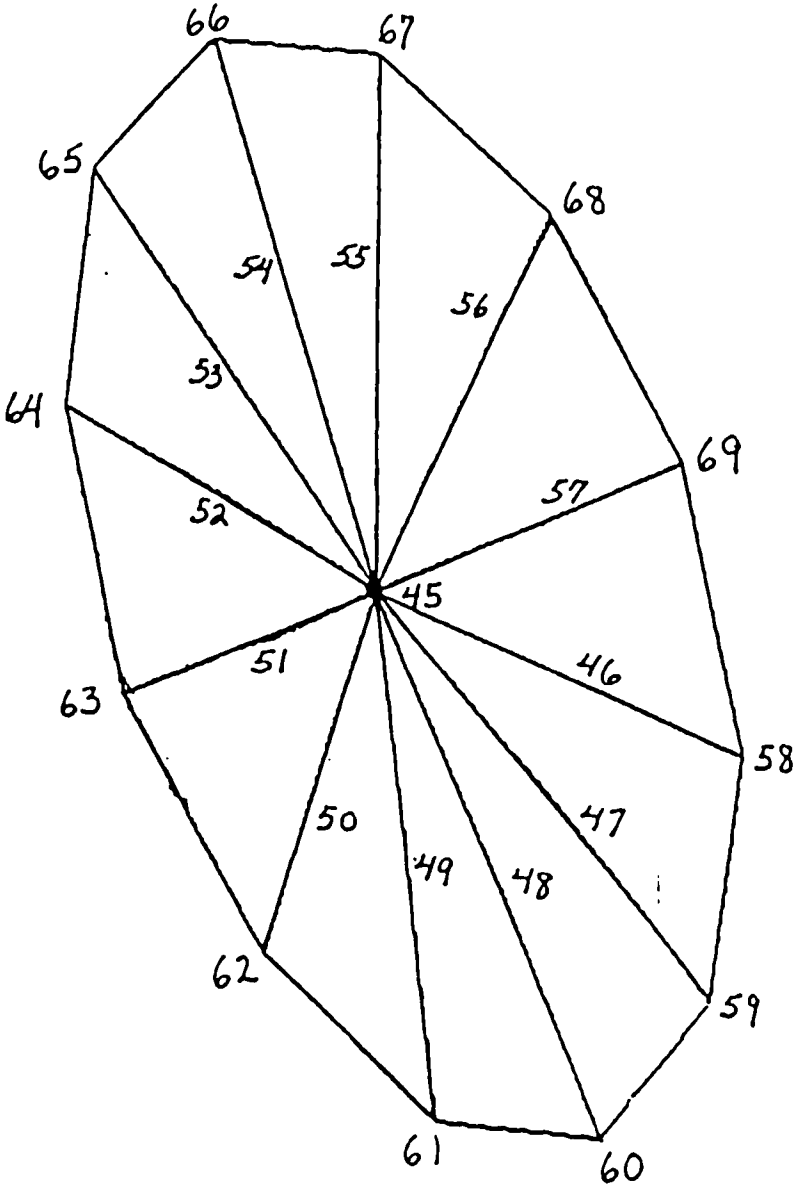

15 M Antenna

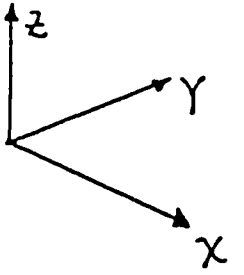

Figure 2. EPS Antenna Nodes

Key results are presented in the Simulation Results section.

A second actuator placement algorithm has also been studied; it is based on the concept of the "degree of controllability" (DOC). However, because of time constraints, no simulation results were obtained.

Optimal Rigid-Body Open-Loop Control

The rigid body equations of motion are given by a set of nonlinear differential equations, and the nominal rigid-body control is specified by the minimization of a finite-time performance index subject to specified initial and final conditions. The solution for the rigid-body open-loop control thus requires the solution to a nonlinear two-point boundary-value problem. The solution approach is identical to that described in Chun and Turner, 1988 and will only be briefly described here.

While there are many methods for solving nonlinear two-point boundary-value problems (TPBVP), the approach we have chosen employs the continuation or homotopy chain method, since the method is easy to apply, and it has global convergence properties. The continuation method involves the embedding of a parameter into the original problem to form a family of problems in such a way that a simple, easy-to-solve problem is defined when the parameter is set to zero, and the original hard-to-solve nonlinear problem is recovered when the parameter is set to one. In the version of the continuation method that we have chosen, the solution to the easy-to-solve problem is first obtained, and the continuation parameter is slowly incremented from zero to one, sweeping out a series of solutions which culminate in the desired solution of the original nonlinear problem.

State Variables

For the rigid body control problem, let us select angles, angular velocities, torques, and torque rates as the state variables. Here, we concern ourselves with only the rotational degrees-of-freedom, since translational motion is of little consequence for slew maneuvers. The available choices for angular representation are direction cosines, Euler parameters (quarternions), or Euler angles. We choose Euler parameters because it is a unique set of numbers and does not encounter singularities at certain orientations, compared with a set of Euler angles, which is determined from one of twelve possible Euler sequences and exhibits "gimbal lock" at certain orientations. Direction cosines are also not chosen as state variables because of the larger number of variables needed. Body angular velocities are used as the velocity variables, and the torque variables

are normalized by the moment of inertia matrix.

The Euler parameters (β_0, β_1, β_2, β_3) may be interpreted geometrically in terms of Euler's theorem which states: An arbitrary reorientation of a rigid body can be accomplished by a single rotation of the body about the principal line $\hat{I}$ through the angle ϕ. In terms of $\hat{I}$ and ϕ, the Euler parameters are expressed as

$$\left.\begin{aligned} \beta_0 &= \cos\frac{\phi}{2} \\ \beta_i &= l_i \sin\frac{\phi}{2},\ i=1,2,3 \end{aligned}\right\} \tag{9}$$

It is clear from the above expressions that the Euler parameters satisfy the constraint

$$\sum_{i=0}^{3} \beta_i^2 = 1 \tag{10}$$

and hence are a once-redundant set of variables.

The Euler parameter rates are related to the body angular velocities by the equations

$$\dot{\beta} = \Omega(\omega)\beta \tag{11}$$

where

$$\Omega(\omega) = \frac{1}{2}\begin{bmatrix} 0 & -\omega_x & -\omega_y & -\omega_z \\ \omega_x & 0 & \omega_z & -\omega_y \\ \omega_y & -\omega_z & 0 & \omega_x \\ \omega_z & \omega_y & -\omega_x & 0 \end{bmatrix}$$

The differential equation for the body angular velocities is derived from Euler's equation, and is given by

$$\dot{\omega} = u_0 + G(\omega) \tag{12}$$

where

$$G(\omega) = -[I]^{-1}[\tilde{\omega}][I]\omega$$

and $[I]$ is the moment of inertia matrix.

The normalized torques and torque rates are included as state variables so as to incorporate frequency-shaping of the torque profile. The torque vector is normalized by the inertia matrix because this reduces the range of numerical values between the states and costates of the resulting optimal control problem. The normalized torque vector u_0, which has units of rad/sec^2, is related to the physical torque vector by the expression

$$u_0 = [I]^{-1}\begin{Bmatrix} u_x \\ u_y \\ u_z \end{Bmatrix}$$

where $[u_x, u_y, u_z]$ is the physical torque vector. The differential equations for the normalized torques and torque rates are given by:

$$\dot{u}_0 = u_1 \tag{13}$$

and

$$\dot{u}_1 = u_2 \tag{14}$$

Optimal Control Definition

We define the optimal control problem for arbitrary frequency-shaped three-axis maneuvers of a general rigid body by the minimization of the following finite-time quadratic performance index:

$$J = \frac{1}{2}\int_{t_o}^{t_f}[\chi^T(t)\ u_2^T(t)]W\begin{Bmatrix} \chi(t) \\ u_2(t) \end{Bmatrix} dt \tag{15}$$

where the state vector is defined as

$$\chi = [\beta^T\ \omega^T\ u_0^T\ u_1^T]^T$$

the control variable is defined as u_2, and the weight matrix is defined as

$$W = \begin{bmatrix} 0 & 0 & 0 & 0 & 0 \\ 0 & Q & 0 & 0 & 0 \\ 0 & 0 & I & 0 & I/\omega_B^2 \\ 0 & 0 & 0 & 0 & 0 \\ 0 & 0 & I/\omega_B^2 & 0 & I/\omega_B^4 \end{bmatrix}$$

The minimization is to be carried out subject to the state differential equations given by Eqs. (11)-(14), and specified initial and final states. The symbol I represents the (3×3) identity matrix. The form of the penalties on the normalized torque and torque rates reflects the time-domain equivalent of a frequency-domain penalty on the normalized torque (see Gupta, 1980). This penalty produces a two pole roll-off of the normalized torque's frequency content at the break frequency, ω_B, and also allows the torque and torque rate to be specified at the initial and final times. A weighting penalty is placed on the angular velocities but not on the Euler parameters because the latter are allowed to be large.

The costate differential equations can be shown to be given by:

$$\dot{\gamma} = \Omega(\omega)\gamma \tag{16}$$

$$\dot{\lambda} = -Q\omega - B^T\gamma + \{[I\omega]\} \times [I]^{-1}\lambda - [I][\tilde{\omega}][I]^{-1}\lambda \tag{17}$$

$$\dot{\mu}_0 = - u_0 - u_2/\omega_B^2 - \lambda \tag{18}$$

$$\dot{\mu}_1 = -\mu_0 \tag{19}$$

where $\gamma(4\times1)$, $\lambda(3\times1)$, $\mu_0(3\times1)$, and $\mu_1(3\times1)$ are costate or adjoint variables for β, ω, u_0, and u_1, respectively. The optimal control vector, which is the second time derivative of the normalized torques, is given by

$$u_2 = -\omega_B^4[\mu_1 + u_0/\omega_B^2] \tag{20}$$

Solution of the Nonlinear Optimal Control Problem

The necessary conditions given by Eqs. (16)-(19) and the associated initial and final conditions represent a nonlinear TPBVP. The solution approach that we have taken employs the continuation method, whereby continuation parameters are embedded into the original nonlinear TPBVP to form a family of intermediate problems in such a way that a simple problem is defined when the parameters are set to zero and the original nonlinear TPBVP is recovered when the parameters are set to one.

The simple problem that we have chosen is a single-axis maneuver about a principal axis of inertia, since its solution is known in closed form. To obtain this simple problem, we introduce a continuation parameter, α_1, that multiplies the off-diagonal terms of the inertia matrix:

$$[I(\alpha_1)] = \begin{bmatrix} I_{xx} & -\alpha_1 I_{xy} & -\alpha_1 I_{xz} \\ -\alpha_1 I_{yx} & I_{yy} & -\alpha_1 I_{yz} \\ -\alpha_1 I_{zx} & -\alpha_1 I_{zy} & I_{zz} \end{bmatrix}$$

which we will call the modified inertia matrix. We also introduce a second continuation parameter, α_2, that multiplies the terminal angles, angular velocities, normalized torques, and torque rates along two of the three coordinate axes. The remaining coordinate axis is the selected axis about which the single-axis starting guess is to be computed. These will be called the modified boundary conditions. A modified TPBVP is defined when the modified inertia matrix is substituted into the nonlinear state-costate differential equations in conjunction with the modified boundary conditions.

A separate set of minimum-state optimal control equations can be generated which correspond to the continuation-modified maneuver problem with the continuation parameters set to zero. The solution of the state-costate differential equations for this problem can be expressed in the exponential matrix form

$$\chi(t_f) = e^{K(t_f - t_0)}\chi(t_0) \tag{21}$$

where χ is the augmented state-costate vector and K is the Hamiltonian matrix. The linear TPBVP can be solved by the standard partitioned matrix solution, yielding the initial costates (Chun, 1986). The initial angle and initial angular costate can then be mapped into the corresponding two Euler parameters

and two Euler parameter costates for the continuation-modified problem with zero continuation parameters (p. 54, Chun and Turner, 1988). The other variables - angular velocities, normalized torque, normalized torque rate, and their costate variables are mapped directly. All other state and costate variables of the nonlinear problem are set to zero at the initial time.

The continuation of the simple problem to the original problem then proceeds as follows:

1. Increment α_1 and α_2. Compute the corresponding modified inertia matrix and modified boundary conditions.
2. Integrate the modified nonlinear state-costate differential equations and sensitivity matrices.
3. Compute the terminal error.
4. If the terminal error is large, apply corrections to the initial costates and go to Step 2.
5. If $\alpha_1 = 1$, and $\alpha_2 = 1$, stop. The nonlinear solution has been found.
6. Go to Step 1.

Details on the calculation of the sensitivity matrices and the initial costate corrections can be found in Chun, 1986.

Closed-Loop Perturbation Feedback Controller

Since the open-loop optimal control is designed with a rigid model of the structure, direct application of the nominal control profile on the flexible structure will lead to errors in the maneuver angle as well as unwanted vibrations. To suppress these errors, a closed-loop perturbation feedback controller is designed to apply corrective torques and forces on the flexible structure to cause it to follow the nominal rigid body profile as closely as possible. The control design closely follows the approach described in Chun and Turner, 1988, with the exception of an added disturbance rejection to account for elastic response due to applied nominal torques.

Control Design Strategy

A reduced order model for the flexible plant is selected based on the response of the full order flexible plant to the open-loop nominal torques. Since the nominal torques are determined from a frequency-shaped control

formulation, the number of modes that are excited by the nominal torques is small, thus requiring only a small number of modes for the reduced order model.

Since the plant dynamics is nonlinear during the large-angle rapid maneuver, we choose a piecewise-linear quasistatic approach to the control design so that standard linear quadratic regulator (LQR) techniques can be applied. The nonlinear flexible plant is linearized at several points along the nominal trajectory, and constant LQR feedback gains are calculated for each of the linearized plants. The number of linearization points to be used depends on the 'strength' of the nonlinearities.

Frequency-shaping is also used in the design of the feedback controller to minimize the possibility of control spillover. A disturbance-rejection feedforward is introduced to reduce the amount of excitation of the elastic modes that is caused by application of the nominal torques. Gain scheduling during the actual maneuver is performed by interpolating the LQR feedback and feedforward gains between the linearization times.

Control Problem Formulation

Flexible plant linearization is performed numerically by DISCOS (Dynamic Interaction Simulation of Controls and Structures), which uses finite differences and quadratic fits to obtain the linearized plant dynamics and control influence matrices. The linearization is performed about the nominal rigid body trajectory at several equally spaced intervals in time.

For each linearized plant, a set of feedback and feedforward gains are obtained from a frequency-shaped LQR design. Specifically, we seek to minimize a performance index of the form:

$$J = \frac{1}{2}\int_{t_0}^{\infty} [\delta x^T(t) \quad \delta u_0^T(t) \quad \delta u_1^T(t) \quad \delta u_2^T(t)]\, W \begin{Bmatrix} \delta x(t) \\ \delta u_0(t) \\ \delta u_1(t) \\ \delta u_2(t) \end{Bmatrix} dt \qquad (22)$$

where

$$W = \begin{bmatrix} \tilde{Q} & N \\ N^T & R \end{bmatrix} \qquad \tilde{Q} = \begin{bmatrix} Q & 0 & 0 \\ 0 & D & 0 \\ 0 & 0 & 0 \end{bmatrix}$$

$$N^T = [0 \quad D/\omega_B^2 \quad 0] \qquad R = D/\omega_B^4$$

δx is a vector of rigid and elastic modal perturbations, δu_0 is a vector containing actuator forces and perturbations of normalized torques, and δu_1, δu_2 are the first and second derivatives of δu_0. The form of the weighting terms on the control-related states reflects the use of frequency-shaping which penalizes the frequency content of the controls that are above the break frequency, ω_B.

Minimization of the above performance index is carried out subject to the following differential equation constraints which describe the reduced order flexible structure and frequency-shaped controls:

$$\delta\dot{X}(t) = \bar{A}\delta X(t) + \bar{B}\delta u_2(t) + \bar{d}(t) \tag{23}$$

where

$$\bar{A} \triangleq \begin{bmatrix} A^{(i)} & B^{(i)} & 0 \\ 0 & 0 & I \\ 0 & 0 & 0 \end{bmatrix}, \qquad \bar{B} \triangleq \begin{Bmatrix} 0 \\ 0 \\ I \end{Bmatrix}$$

$$\delta X \triangleq \begin{Bmatrix} \delta x \\ \delta u_0 \\ \delta u_1 \end{Bmatrix}, \qquad \bar{d} \triangleq \begin{Bmatrix} d \\ 0 \\ 0 \end{Bmatrix}$$

In the above expression, $A^{(i)}$ and $B^{(i)}$ are the linearized system dynamics and control influence matrices, respectively, and $d(t)$ is a vector of arbitrary disturbances.

Application of Pontryagin's Principle leads to necessary conditions consisting of the following state and costate differential equations:

$$\delta\dot{X} = [\bar{A}-\bar{B}R^{-1}N^T]\delta X - \bar{B}R^{-1}\bar{B}^T\lambda + \bar{d} \tag{24}$$

$$\dot{\lambda} = -[\bar{A}^T-NR^{-1}\bar{B}^T]\lambda - [Q-NR^{-1}N^T]\delta X \tag{25}$$

and the following optimal control equation:

$$\delta u_2 = -R^{-1}[\bar{B}^T\lambda+N^T\delta X] \tag{26}$$

One can assume a feedback/feedforward solution of the form

$$\lambda(t) = P(t)\delta X(t) + \xi(t) \tag{27}$$

which, upon substitution into the necessary conditions, yields the following equations for the gain variables at steady state:

$$\dot{P} = 0 = -P\tilde{A} - \tilde{A}^T P + [P\tilde{B}+N]R^{-1}[N^T+\tilde{B}^T P] - Q \tag{28}$$

$$\dot{\xi} = 0 = -[\tilde{A}-\tilde{B}R^{-1}(\tilde{B}^T P+N^T)]^T\xi - P\tilde{d} \tag{29}$$

The optimal feedback/feedforward control can then be given by the expression:

$$\begin{aligned}\delta u_2(t) &= -R^{-1}(\tilde{B}^T P_{ss}+N^T)\delta X(t) \\ &+ R^{-1}\tilde{B}^T[\tilde{A}^T-(P_{ss}\tilde{B}+N)R^{-1}\tilde{B}^T]^{-1}P_{ss}\tilde{d}(t)\end{aligned} \tag{30}$$

where the disturbance is assumed to be slowly-varying.

Disturbance Vector

The disturbance vector $d(t)$ can be arbitrary. For the purpose of reducing the amount of slew-induced deformations, it is desirable to model the modal forcing term that is due to the nominal slew as a modal disturbance. From the equations of motion, it can be shown that the modal acceleration caused by the nominal slew torques is given by:

$$\ddot{\eta}_n = [0\ \ 0\ \ I]^T \begin{bmatrix} J & -S & d \\ S & m & a \\ d^T & a^T & e \end{bmatrix}^{-1} \begin{bmatrix} I \\ 0 \\ \sigma^T \end{bmatrix} \{u\} \tag{31}$$

where the mass matrix has been partitioned into rotational, translational, and modal parts, and σ is the matrix of modal slopes at the point of application of the torques, u. The disturbance vector $d(t)$ thus contains one non-zero term, given by Eq. (31) in the appropriate row for modal disturbance.

Both 'constant' and time-varying disturbance vectors are tested in the example simulations. In the 'constant' case, the last term in Eq. (30) is evaluated at the linearization times and interpolated during the maneuver. In the time-varying case, the feedforward gains (coefficients of $\tilde{d}(t)$ in Eq. (30)) are interpolated during the maneuver, but the disturbance vector itself is calculated at each moment using Eq. (31).

Force/Torque Decoupling

One of the observations that can made from the simulation runs was that the additional use of force actuators for the perturbation feedback controller leads to an increase in the torque levels and correspondingly large force levels. What appears to be happening is that the actuator forces produce moment couples which oppose the applied torques. One way of alleviating this is to utilize the force actuators to contribute to the required nominal torque profile (in addition to the torquers) using a torque-proportioning algorithm that reduces the amount of induced elastic deformation. An additional approach is to constrain the actuator forces so as not to produce any net torques. The control forces will then be able to affect only the flexible response (as well as translation). This approach is briefly outlined as follows.

For frequency-shaped controls, the decoupling constraint can be imposed on the highest derivative of the forces that appears in the control formulation (assuming zero initial conditions). The constraint to be applied can be expressed by the equation:

$$\sum_i \tilde{r}_i f_i = 0 \tag{32}$$

where r_i is the vector from the center of mass to the force actuator location, the tilde represents a skew-symmetrized matrix, and f_i is the highest derivative of the applied force. Each force derivative resides in a partition of the control vector, and is therefore related to the control vector by the selection matrix, S_i:

$$f_i = S_i u$$

On appending the decoupling constraint to the performance index, the resulting necessary condition for control optimality is:

$$u_2 = -R^{-1}[\tilde{B}^T \lambda + N^T \delta X + W\kappa] \tag{33}$$

where

$$W \triangleq \sum_i \tilde{r}_i S_i$$

and κ is a 3×1 vector of Lagrange multipliers for the decoupling constraint. Substitution of this control expression into the decoupling constraint yields the solution for κ:

$$\kappa = -[WR^{-1}W^T]^{-1}WR^{-1}(\tilde{B}^T\lambda + N^T\delta X) \tag{34}$$

Assuming the feedback/feedforward form of Eq. (27), the steady-state gain expressions become:

$$\dot{P} = 0 = -P\hat{A} - \hat{A}^TP + [P\tilde{B} + N]\hat{R}^{-1}[N^T + \tilde{B}^TP] - \hat{Q} \tag{35}$$

$$\dot{\xi} = 0 = -[\hat{A} - \tilde{B}\hat{R}^{-1}(\tilde{B}^TP + N^T)]^T\xi - P\tilde{d} \tag{36}$$

where

$$\hat{R} = R + \tfrac{1}{2}W^T(WR^{-1}W^T)^{-1}W$$

$$\hat{A} = \tilde{A} - \tilde{B}\hat{R}^{-1}N^T$$

$$\hat{Q} = Q - N\hat{R}^{-1}N^T$$

The final control vector is then given by the expression

$$\begin{aligned} u_2 = &-\hat{R}^{-1}[\tilde{B}^TP_{ss} + N^T]\delta X \\ &+ \hat{R}^{-1}\tilde{B}^T[\hat{A}^T - P_{ss}\tilde{B}\hat{R}^{-1}\tilde{B}^T]^{-1}P_{ss}\tilde{d} \end{aligned} \tag{37}$$

Extension to Class IV Missions

The control approach that has been applied to the Class III mission can easily be adapted for the Class IV mission. Modifications to the approach include the use of multibody dynamics equations instead of Euler's equations for the calculation of nominal controls. Partial differentiation of the multibody equations would then provide the appropriate costate differential equations. An Order (n) algorithm (where n is the number of bodies) would reduce the CPU

requirements when the number of bodies is large (Chun, Turner, Frisch, 1989). Since the pointing requirements for the appendages would normally be in inertial coordinates, and the multibody equations are generally in relative coordinates, it is necessary to perform a transformation from inertial to relative coordinates in order to specify the desired terminal conditions.

Another modification to the algorithm would involve expanding the disturbance rejection to account for the effects of interaction forces/torques as well as the nominal maneuver controls. The perturbation controller would feed back the relative appendage motions, in addition to the absolute base body motion and the elastic degrees-of-freedom.

SIMULATION RESULTS AND OBSERVATIONS

The EPS large angle slew maneuver is simulated using DISCOS (Dynamics Interaction Simulation of Controls and Structure). In this study, the example maneuver involves a re-orientation from a frame initially aligned with the inertial frame to a frame that is rotated 1 radian about all three Euler axes. The Euler sequence is arbitrarily chosen to be 1-2-3. Both torquers-only and torquers-plus-force-actuators control are simulated for performance comparisons.

Slew maneuver times of 6 s and 10 s are considered, which are respectively 1.45 and 2.42 times the period of the first elastic mode. The purpose of the shorter 6 s slew is to investigate the effects on response when there is more interaction between the elastic modes and the control torques.

To evaluate the performance of the different simulation cases and to serve as a guideline for the selection of weighting matrices, the following performance goals are established.

(1) Angular errors less than 3% of the desired maneuver angle (1 rad for each Euler axis) after 125% of the nominal rigid body maneuver time has elapsed.
(2) Peak elastic displacement at antenna rim less than one tenth of the open-loop values after 125% of the nominal rigid body maneuver time has elapsed.
(3) Elastic displacements and control efforts minimized during the maneuver.

These performance goals are based on results of preliminary open- and closed-loop simulations.

The 10 s maneuver results are presented first, followed by the more stressing 6 s maneuvers. Open- and closed-loop results are shown for both maneuver times. All of the simulated perturbation controllers use a 'constant' disturbance rejection, unless otherwise stated. See the section on Disturbance Vector on page 18 for details.

Rigid Body Response to 10 s Open-Loop Torque Profile

Figure 3 shows the response of a rigid EPS model subjected to the nominal rigid body torque profile for a 10 s maneuver. The response should match the desired final conditions exactly because the controlled plant is identical to the plant model used in generating the nominal torque profile. Indeed, the total

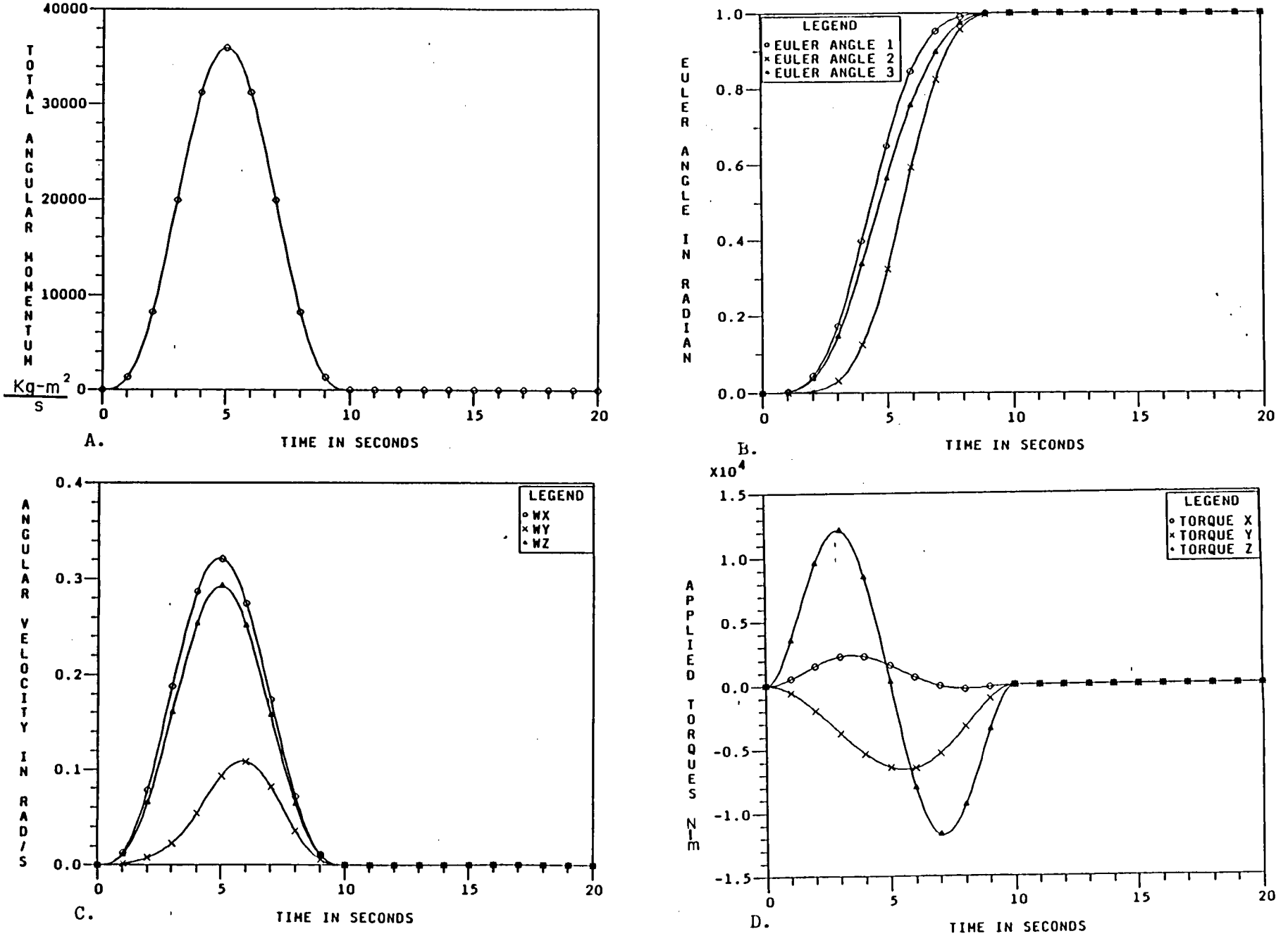

Figure 3. Rigid Body Response to 10 s Open-Loop Torque Profile

angular momentum, Euler angles, angular velocities, and applied torques shown in Fig. 3 reveal that the desired final conditions are attained, thus confirming that the nominal rigid body torque profile is properly computed. The total angular momentum plot shows that the structure's angular momentum increases to a maximum and then decreases back to zero at the end of the maneuver as expected for a rest-to-rest maneuver. The Euler angle plots show that the structure has slewed to 1 radian about all 3 Euler axes at 10 s and stays at that orientation throughout the rest of the simulation. The angular velocities are zero at 10 s and remain at zero. The applied torques are smooth and continuous because of the frequency-shaping formulation, which also allows the torques and their slopes to be specified at the initial and final times. These quantities are set to zero for continuity and smoothness. The peak torque is about 12,000 N-m about the body z axis.

Flexible Body Response to 10 s Open-Loop Torque Profile

The first 10 elastic modes are retained in order to observe the response of the flexible structure due to application of the rigid body open-loop control profile. The results of this case are used to establish a baseline for evaluation of the perturbation feedback controller. The Euler angles, body angular velocities, and modal amplitudes are shown in Fig. 4. The modal amplitude plots show that only the first few modes exhibit any significant amount of residual vibration.

The Euler angle time histories show that there is rigid body drift after the end of the maneuver. This is also indicated by the non-zero residuals in all components of the angular velocity vector. This rigid body drift is always expected when an open-loop control profile, designed with a rigid plant model, is applied to a non-rigid plant.

The elastic deformations at nodes 66 and 69 of the large antenna, and nodes 85 and 88 of the small antenna are presented in Fig. 5. The elastic deformations on the small antenna are seen to be generally a factor of 4-5 smaller than the large antenna. All of the responses are dominated by the first and second modes.

Perturbation Control and Reduced Order Model

Since the open-loop controller is designed using rigid body dynamics, the perturbation feedback control is needed to actively suppress the elastic modes and drive the perturbed trajectory as close to the nominal as possible. The weight matrix selection process is iterative, and the submatrices, Q and D, are constrained to be diagonal so as to limit the number of values to be selected.

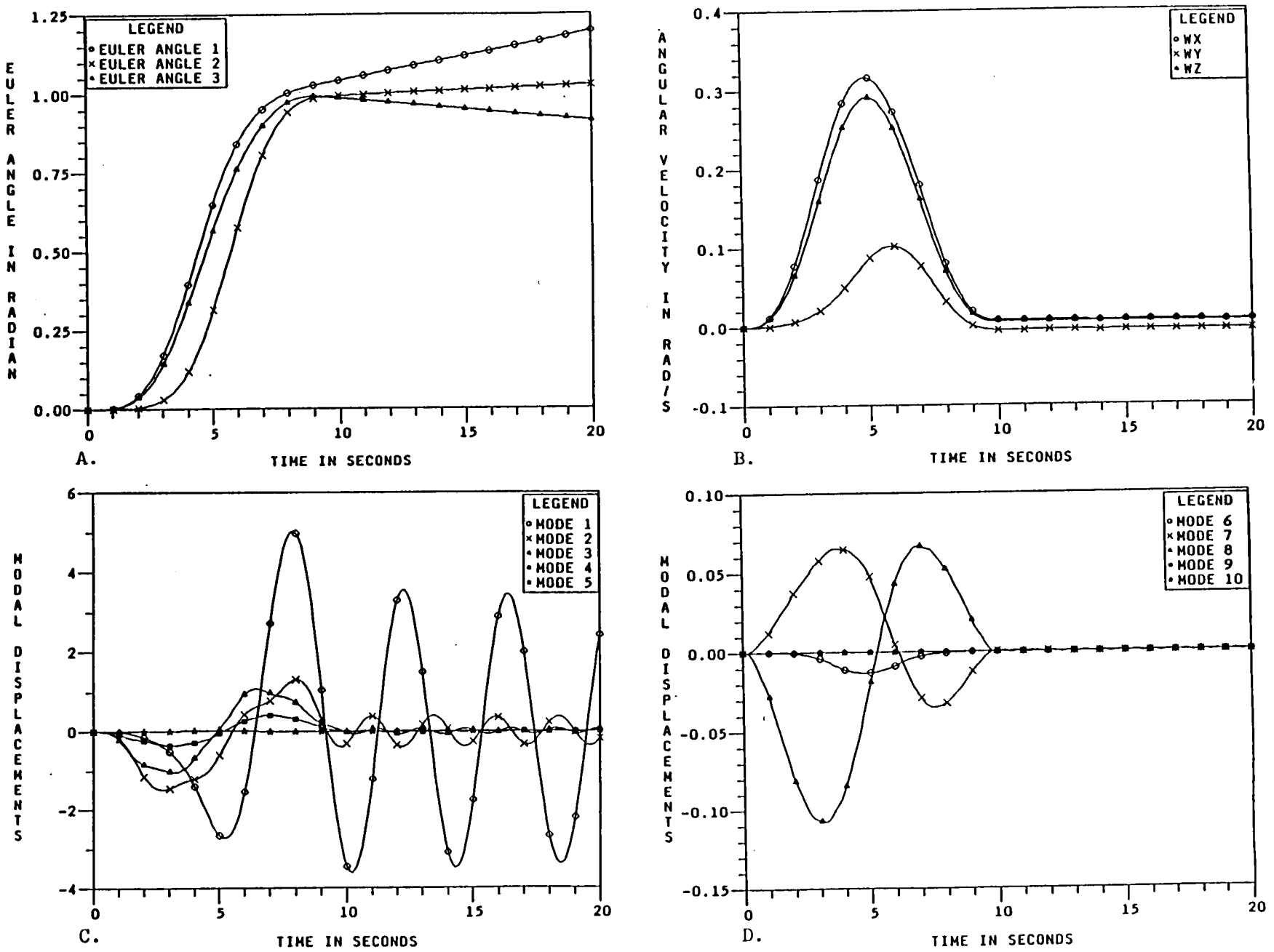

Figure 4. Elastic Response to 10 s Open-Loop Torque, Rotational and Modal

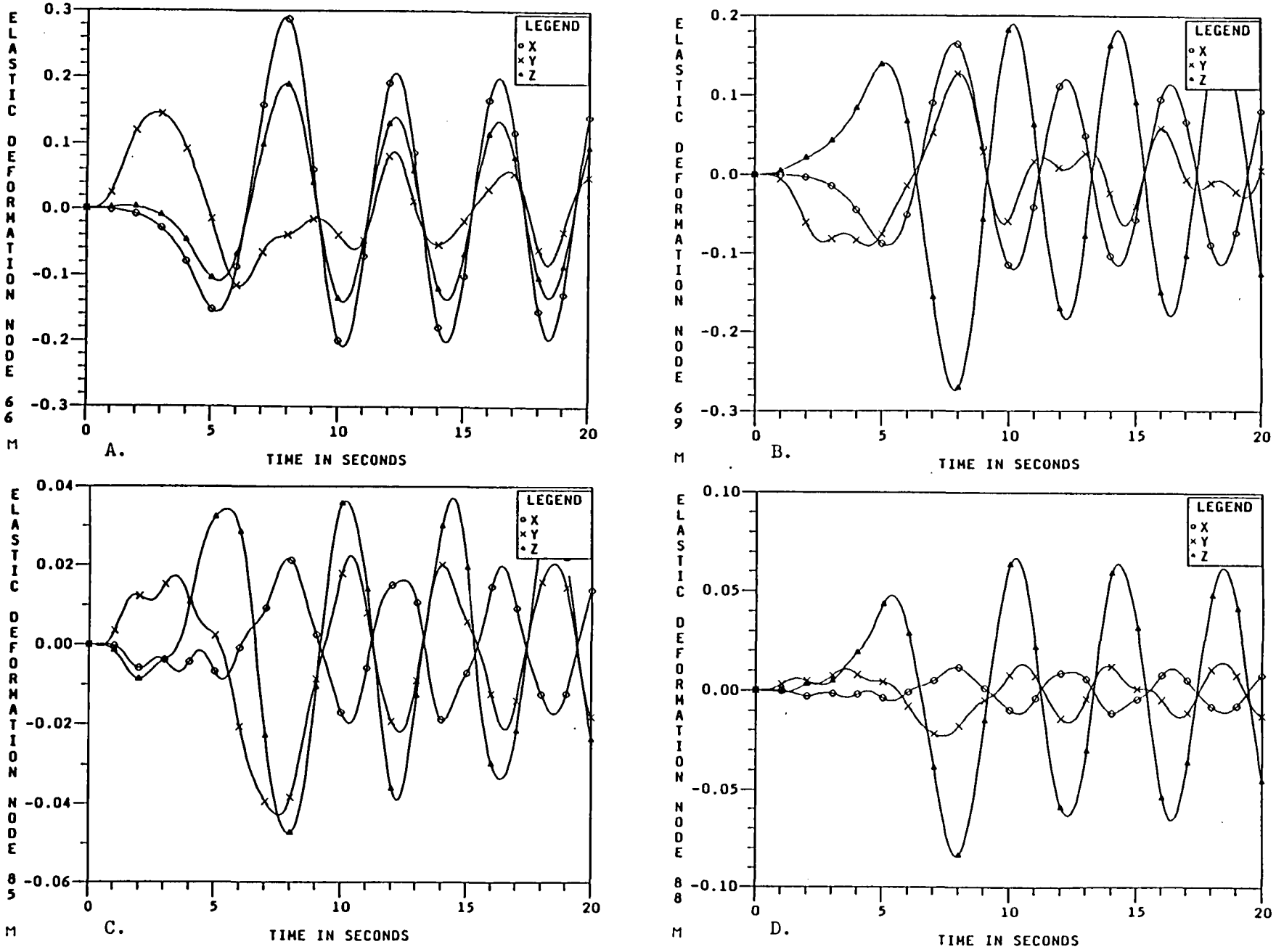

Figure 5. Elastic Response to 10 s Open-Loop Torque, Physical Deformations

For the 10 second slew cases when 45 modes are simulated, the results are similar to the cases where only the first 10 flexible modes are retained. The reduced order perturbation controller is designed using a 10 mode model.

Perturbation Control - Torquers-Only, 10 s Maneuver

The torquers, which are located at the CG of the vehicle, are primarily used to produce the open-loop torques which slew the structure. These torquers are also used by the perturbation controller to control the elastic degrees-of-freedom as well as deviations from the nominal angle trajectory. This case presents the closed-loop response of the flexible plant under perturbation feedback control using torquers as the only actuator device. The open-loop torque profile is designed for a 10 s slew. For this case, the weighting matrices, Q and D, associated with the plant states and control states, respectively, are:

$$Q = \begin{bmatrix} 1000I_3 & 0 & 0 \\ 0 & I_{20} & 0 \\ 0 & 0 & 1000I_3 \end{bmatrix}, \qquad D = \begin{bmatrix} 50 & 0 & 0 \\ 0 & 50 & 0 \\ 0 & 0 & 50 \end{bmatrix}$$

where I_n denotes an $n \times n$ identity matrix. The break frequency, ω_B, is chosen to be 2.5 rad/s. The ordering of the plant states penalized by the weighting matrix Q is given by the angular velocities, modal amplitudes and amplitude rates, and Euler angles. The translational states are ignored.

Figure 6 shows the resulting Euler angle histories and torque perturbations. The Euler angle histories show that the desired orientation is attained after some damped oscillatory response. There is a 10% overshoot in the second Euler angle. The Euler angle errors at 12.5 second are within the 30 mrad performance goal specification. The applied torques are computed as the sum of the nominal torques (Fig. 3d) plus the torque perturbations (Fig. 6b). The peak torque perturbations about each axis are 15-40% of the peak values of the nominal open-loop torques. The largest peak torque perturbation is about 3000 N-m about the y axis. The elastic deformations at nodes 66, 69, 85 and 88 on the antennas are shown in Fig. 7. The elastic deformation of the antennas meets the performance goals after the nominal slew maneuver is completed due to the action of the perturbation feedback controller. During the slew period, the peak elastic deformations at different nodes of the antennas decrease by a factor of 1.5 to 2 when compared with the open-loop values.

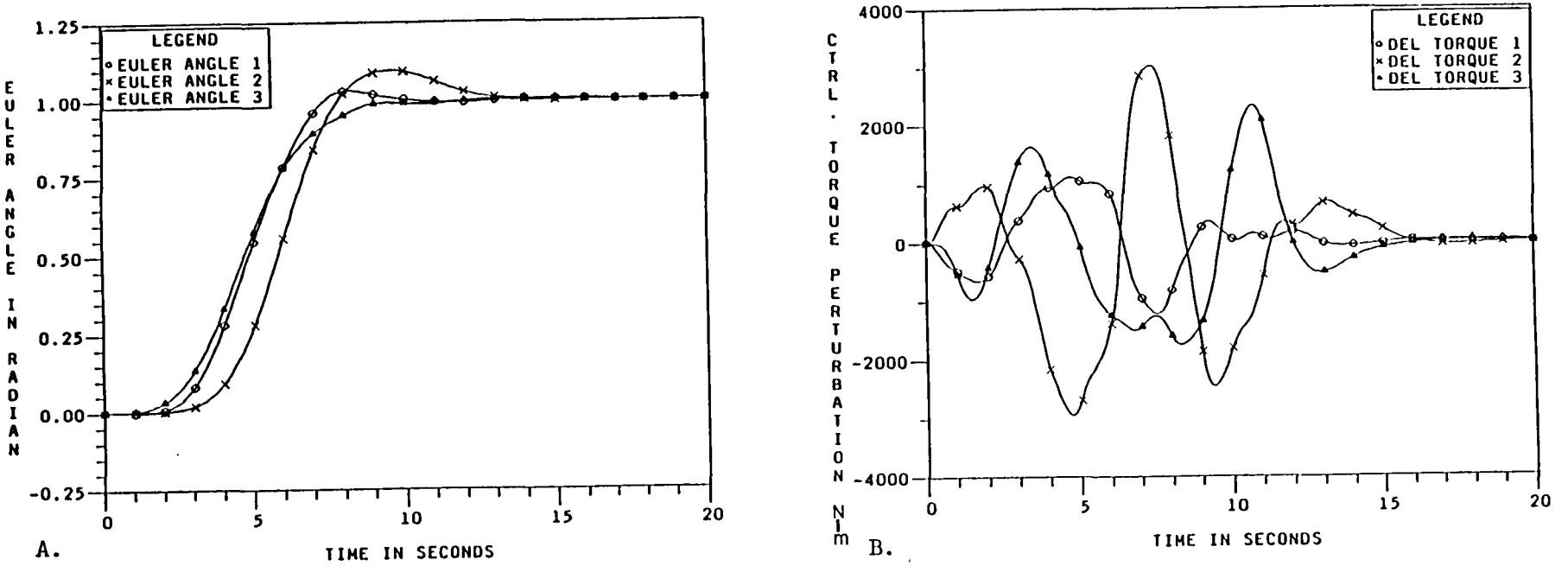

Figure 6. Feedback Control for 10 s Slew, Using Torquers Only

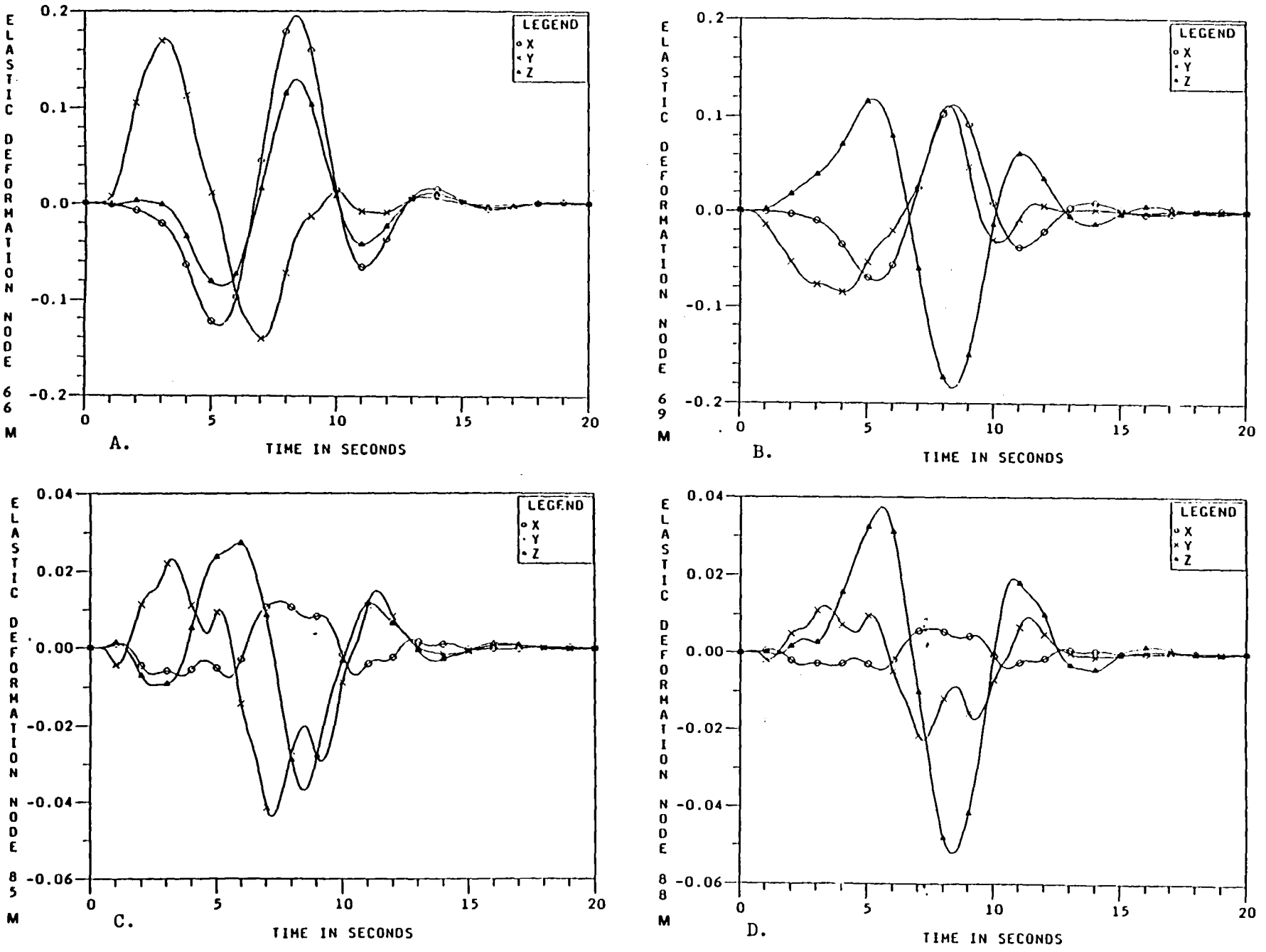

Figure 7. Feedback Control for 10 s Slew, Using Torquers Only

Perturbation Control - Torquers + Force Actuators, 10 s Maneuver

Since the elastic deformations at the outer rims of the antennas are large, it is reasonable to consider placing force actuators at the outer rim to enhance to performance of the perturbation feedback controller. The weighting matrices, Q and D, associated with the plant states and control states, respectively, are as follows:

$$Q = \begin{bmatrix} 1000I_6 & 0 & 0 \\ 0 & Q_a & 0 \\ 0 & 0 & 1000I_6 \end{bmatrix}, \qquad D = \begin{bmatrix} 10I_3 & 0 \\ 0 & 10^{-4}I_7 \end{bmatrix}$$

$$Q_a = \text{DIAG}[25,100,25,7*7.5,25,100,25,7*7.5]$$

In the above expression for Q_a, 7*7.5 indicates that 7.5 is repeated 7 times. The ordering of the plant states is given by the angular velocities, body reference point velocity, modal amplitude and amplitude rates, Euler angles and translational degrees of freedom. The diagonal matrix D penalizes the three control torques and seven actuator forces.

The Euler angles, applied forces, applied torques, and torque perturbations are presented in Fig. 8. The Euler angle histories show that there is more overshoot when compared with the closed-loop torquers-only response (Fig. 6). Nevertheless, the Euler angle errors are within the performance goal. The actuator forces are also quite large as shown in Fig. 8b, where the peak actuator force from one of the actuators is about 70 N. The applied torques and their corresponding torque perturbations are larger than that of the torquers-only case (see Fig. 6). The peak torque perturbation is about 9,000 N-m. This is an indication that there is some degree of interaction between the torquers and the force actuators; the overall effect is a further reduction in the elastic deformations at the antennas' outer rims. The elastic deformations of nodes 66, 69, 85, and 89 are shown in Fig. 9. Compared with the open-loop case, the response of the large antenna is reduced a factor of 5 and response of the small antenna by a factor of 3.

Disturbance Rejection Feedforward

Disturbance rejection feedforward is implemented to counteract the elastic response induced by the rigid body control law. For comparison, the elastic deformations at node 69 of the large antenna are presented in Fig. 10, where the disturbance is modeled as: a) no disturbance, b) piecewise constant, and c) time-varying. The controller configuration is torquers-only, and the open-loop slew

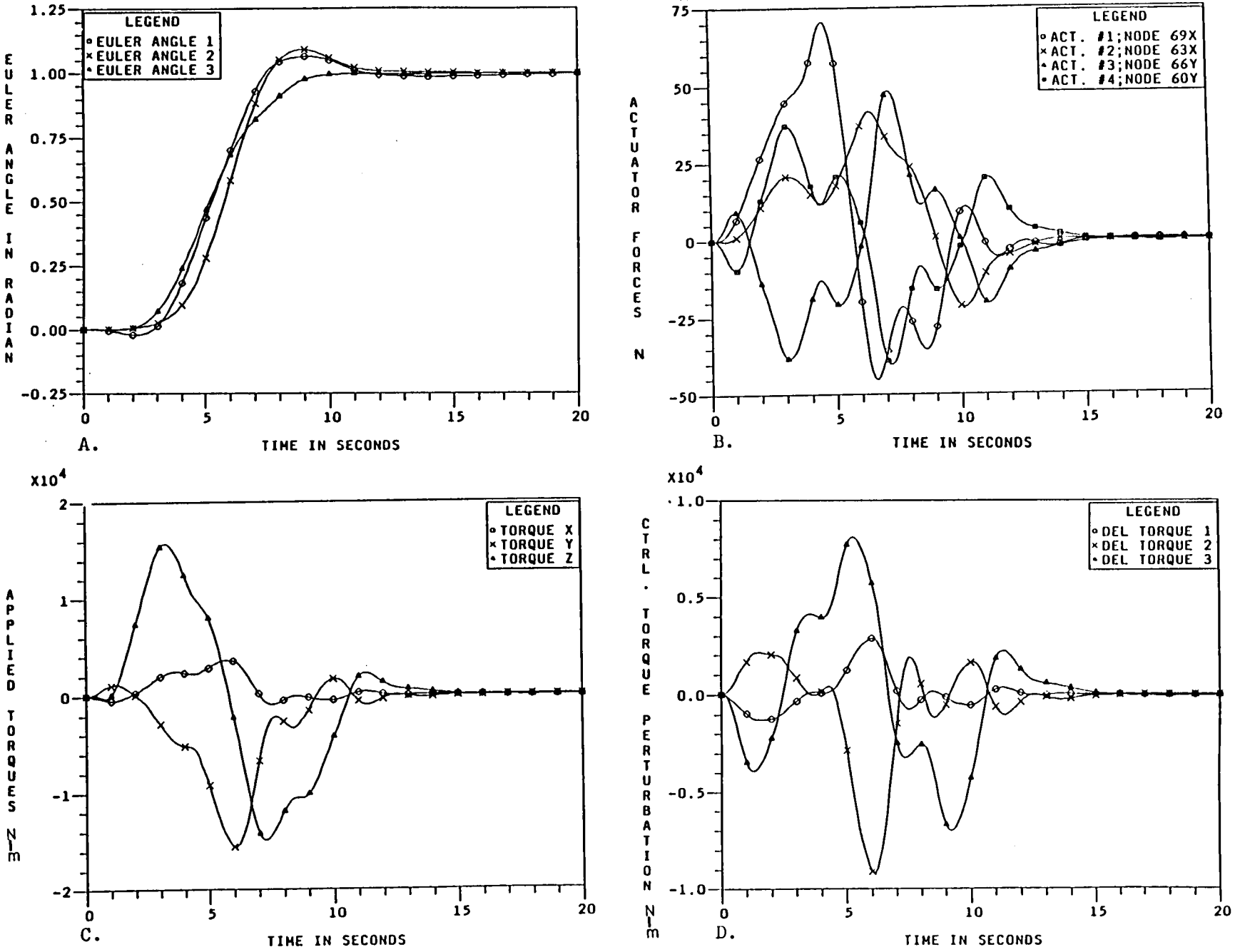

Figure 8. Feedback Control, 10 s Slew, Torquers + Force Actuators

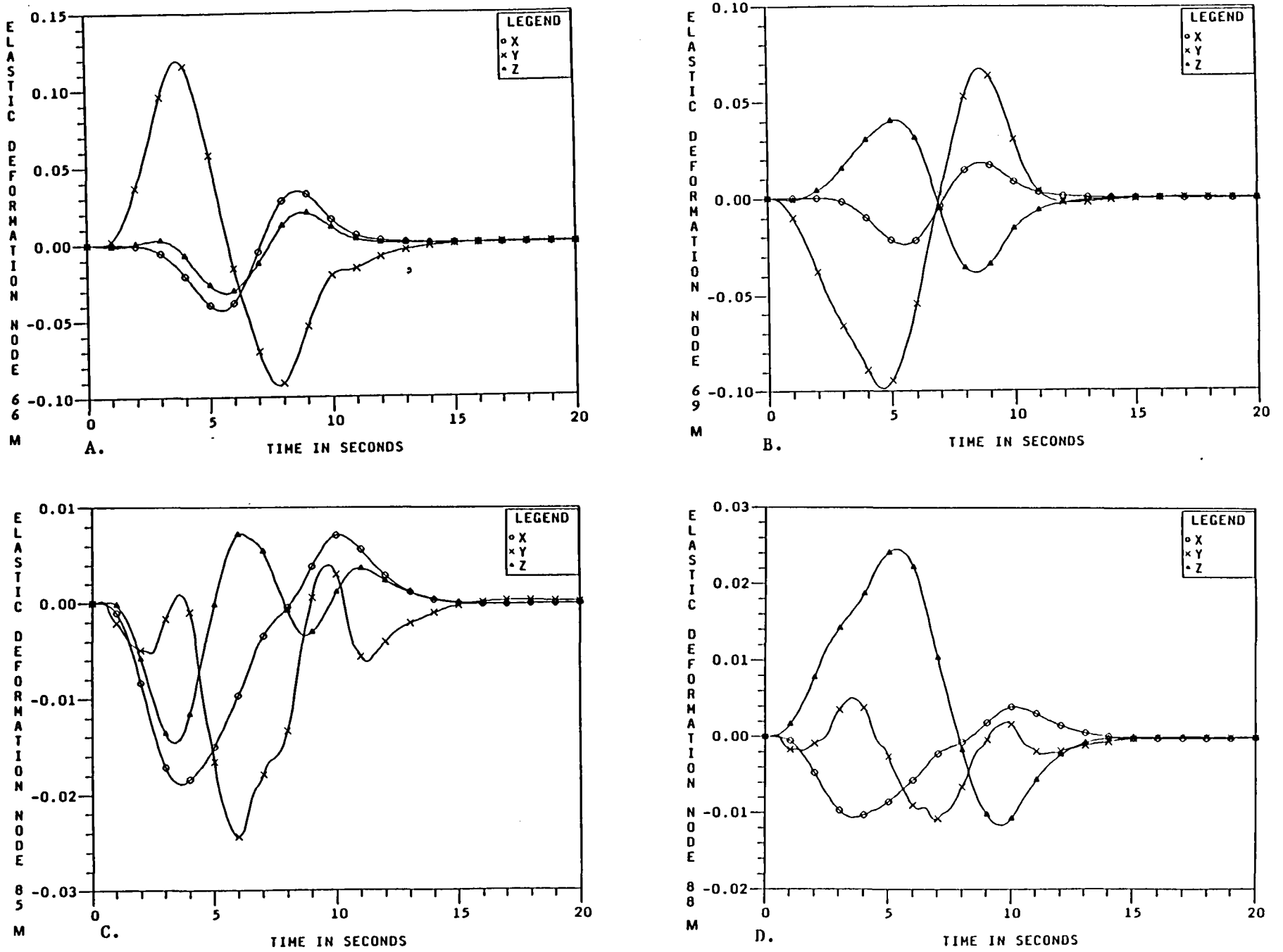

Figure 9. Feedback Control, 10 s Slew, Torquers + Force Actuators

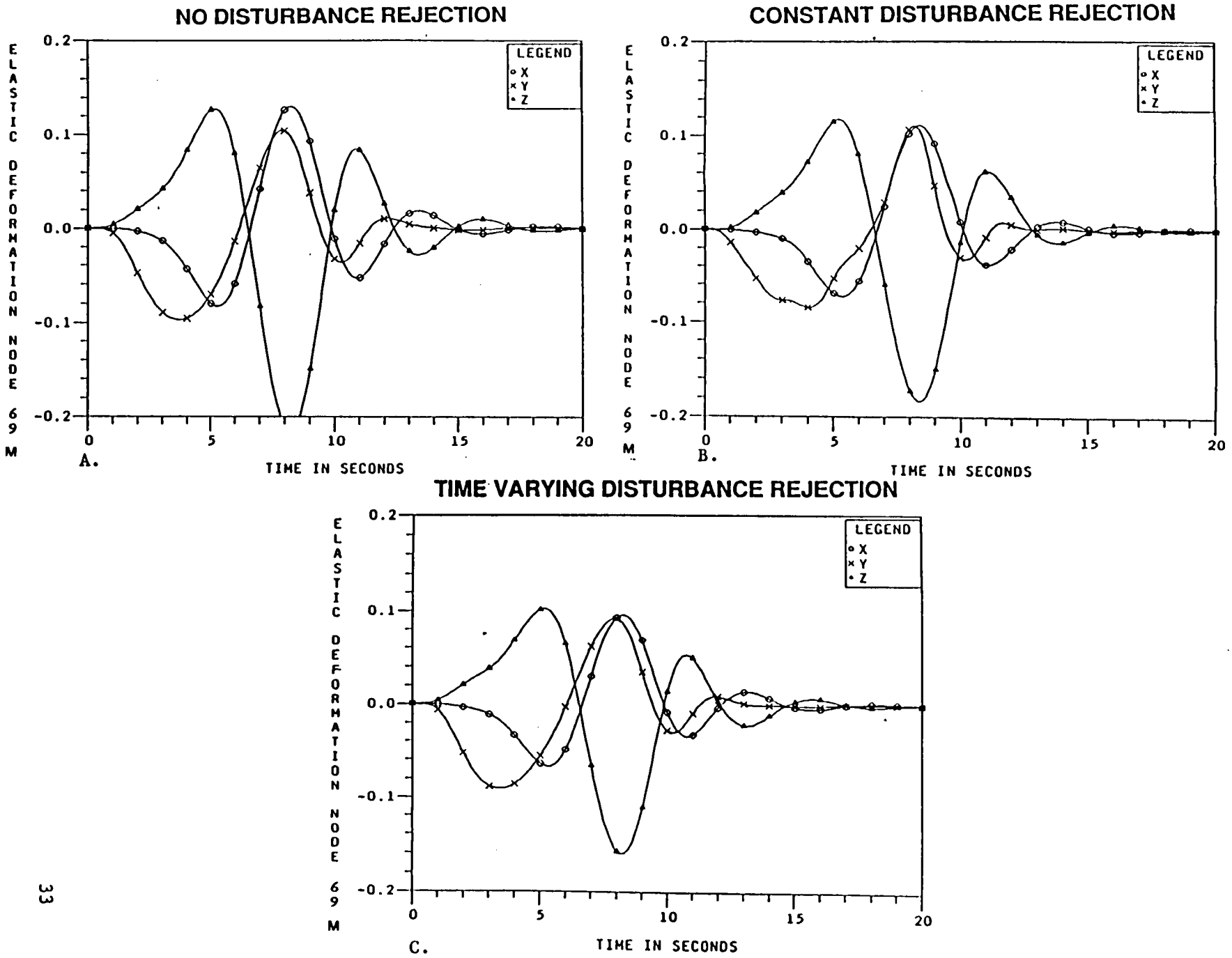

Figure 10. Disturbance Rejection Comparisons

is 10 s. The weight matrices for the states and controls are given by:

$$Q = \begin{bmatrix} 1000I_3 & 0 & 0 \\ 0 & 0.1I_{20} & 0 \\ 0 & 0 & 1000I_3 \end{bmatrix}, \quad D = \begin{bmatrix} 10 & 0 & 0 \\ 0 & 10 & 0 \\ 0 & 0 & 10 \end{bmatrix}$$

It can be seen that the reduction in elastic deformation at this node using time-varying disturbance rejection feedforward can be as large as 30% when compared with the same case without disturbance rejection. Figure 11 shows the Euler angle histories for the case with time-varying disturbance rejection. The Euler angle errors of 5 mrad at 12.5 s are well within the 30 mrad performance goal. The time-varying disturbance rejection case represents the best results obtained for torque-only control.

Flexible Body Response to 6 s Open-Loop Torque Profile

The corresponding maneuver frequency is 0.17 Hz, which is about 70% of the first natural frequency. The 6 s open-loop torque profile is applied to a flexible plant model with all 45 modes retained. The Euler angles and applied torque profile are presented in Fig. 12. The first five modal amplitudes and elastic deformations at nodes 69 and 88 are presented in Fig. 13. The largest slope of the Euler angle errors for this 6 second run is 3-4 times larger than the corresponding 10 s slew case (Fig. 4). The peak modal amplitudes are also about 3-4 times larger than those for the 10 s slew case, while peak elastic deformations at nodes 69 and 88 are 3-5 times larger.

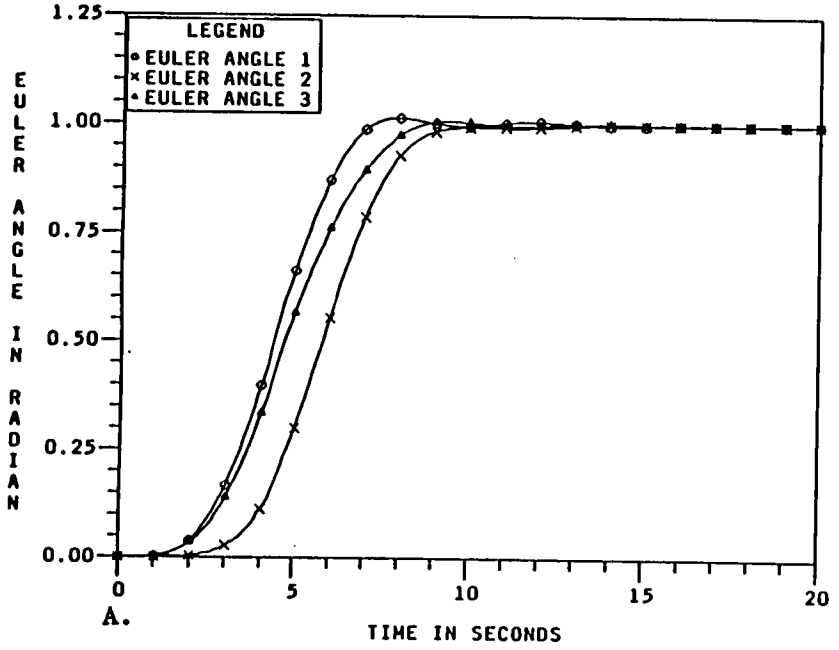

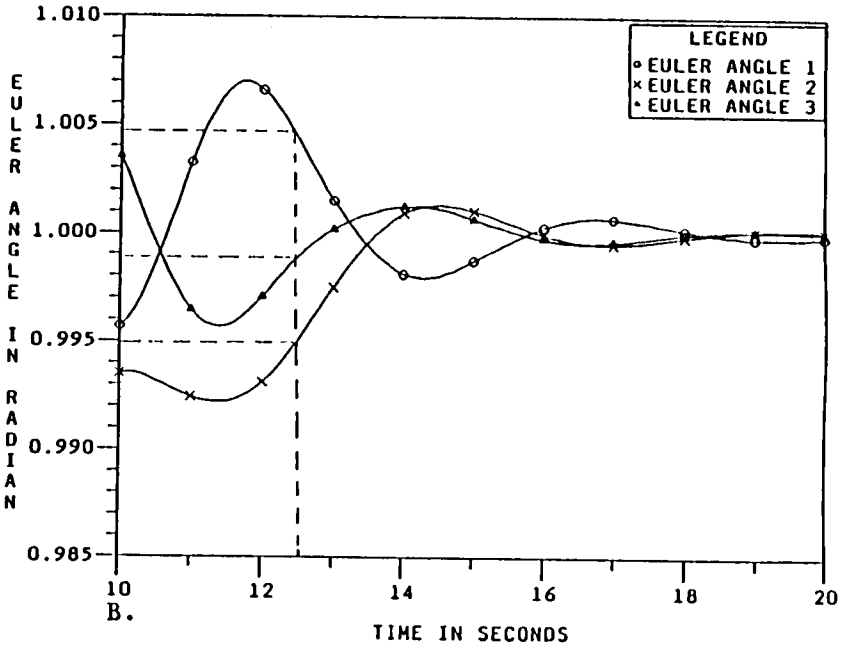

Figure 11. Euler Angles for Time-Varying Disturbance Case

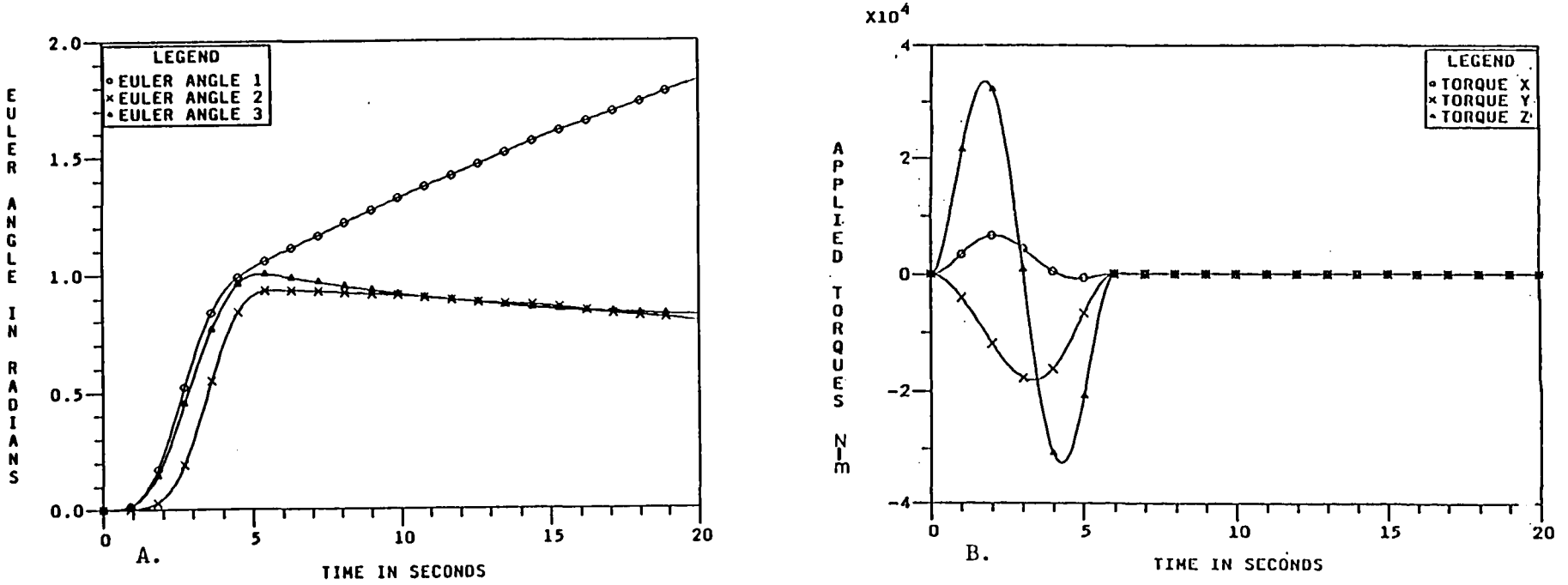

Figure 12. Elastic Response to 6 s Open-Loop Torque

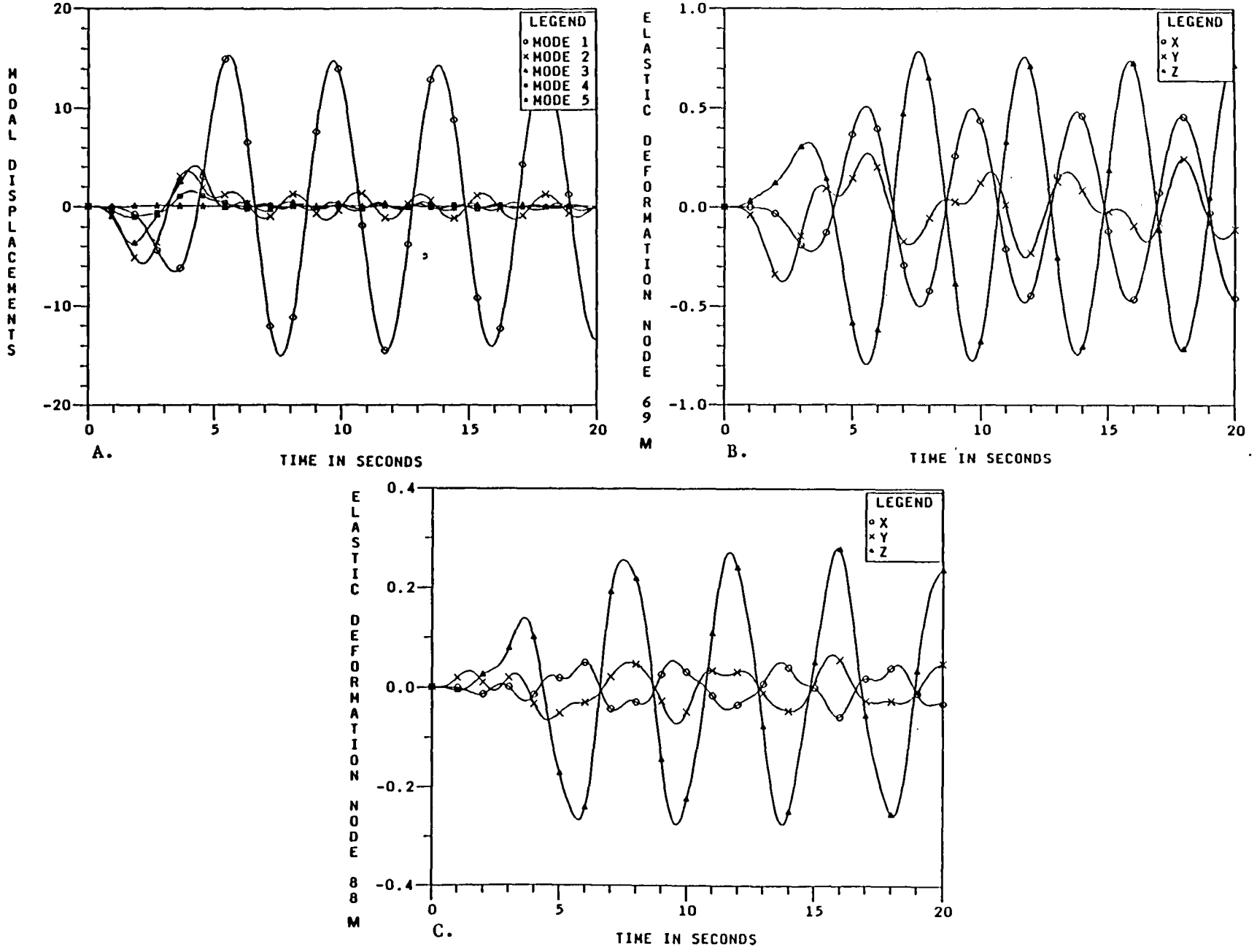

Figure 13. Elastic Response to 6 s Open-Loop Torque Profile

Perturbation Control - Torquers Only, 6 s Maneuver

The perturbation controller is simulated with torques only. Linear translations are ignored for this case. The weighting matrices used are as follows:

$$Q = \begin{bmatrix} 1000I_3 & 0 & 0 \\ 0 & I_{20} & 0 \\ 0 & 0 & 1000I_3 \end{bmatrix} \qquad D = 1000I_3$$

The break frequency is chosen to be 5 rad/s.

The simulation results are shown in Figs. 14 and 15. The Euler angles show a sluggish behavior. At 7.5 s (125% of the elapsed maneuver time), the Euler angle error is about 10-20%, which is outside the performance goal. The peak torque perturbation is about 40% of the largest nominal torque. The deformation magnitudes at the antenna nodes are about 2-3 times larger than the 10 s maneuver, as expected.

Perturbation Control - Torquers + Force Actuators, 6 s Maneuver

The closed-loop response of the perturbation feedback with torquers plus force actuators are shown in Figs. 16 and 17. The break frequency, ω_B, is chosen to be 5.0 rad/s.

Figure 16 indicates that the largest Euler angle error at 7.5 s (125% of the maneuver time) is about 7% of 1 rad, which is outside the desired performance goal, but better than the case with torquers only. There are also overshoots which peak at about $t = 5$ s. The response is sluggish when compared with a similar 10 s slew. A peak force of about 180 N is needed at nodes 60 and 66 versus 80 N needed at nodes 63 and 69. Modal amplitudes of the first 10 modes are presented in Fig. 17. The modal amplitudes of the first 10 modes are considerably reduced after the completion of the nominal slew. The peak elastic deformation during the slew maneuver is observed to be reduced by a factor of about 100:1.

Summary of Simulation Results

The perturbation feedback controller provides a stable and satisfactory closed-loop slew response. In general, the additional use of force actuators yields a slightly better response. However, because of the difficulty in

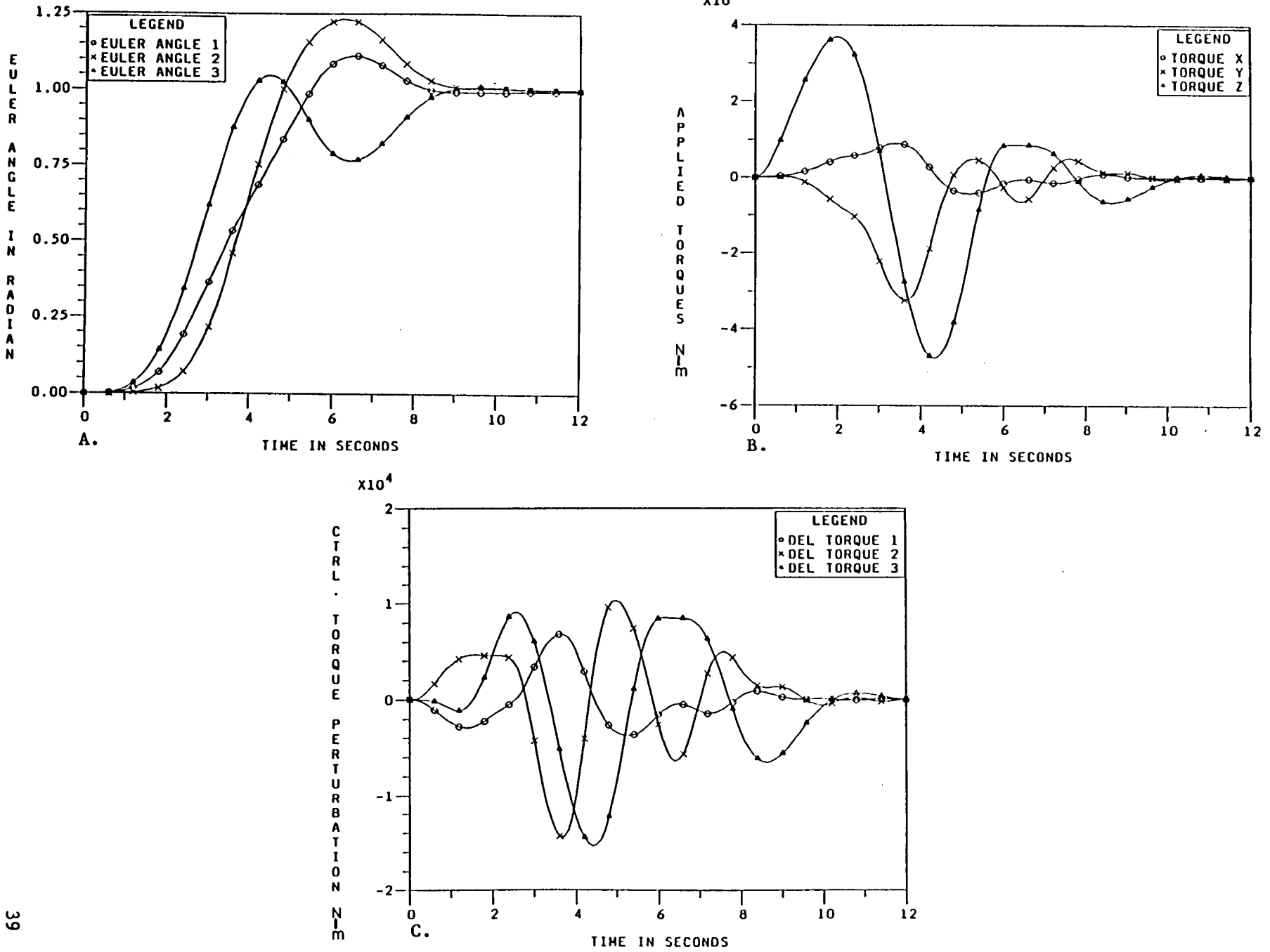

Figure 14. Feedback Control, 6 s Slew, Torquers Only

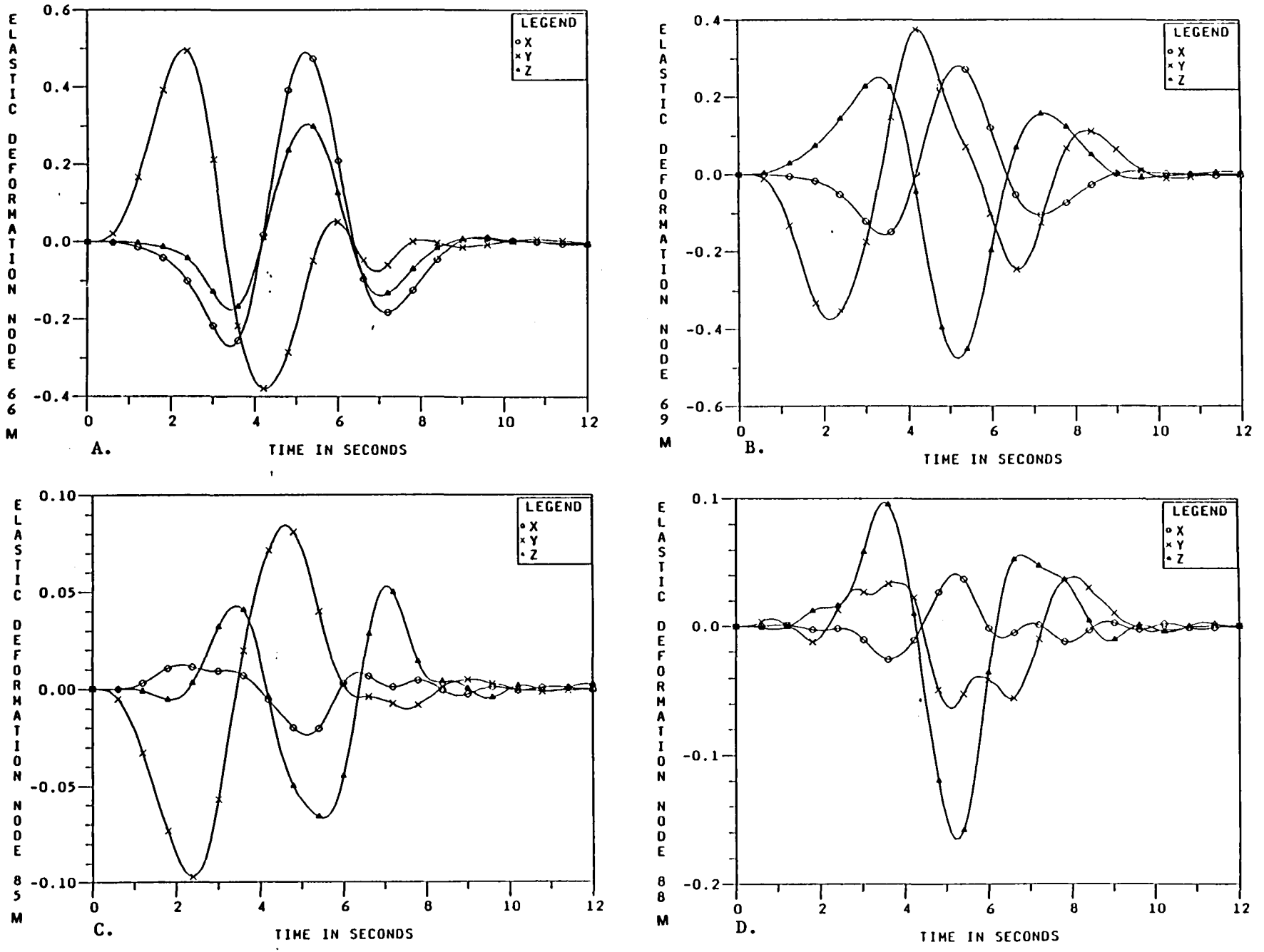

Figure 15. Feedback Control, 6 s Slew, Torquers Only

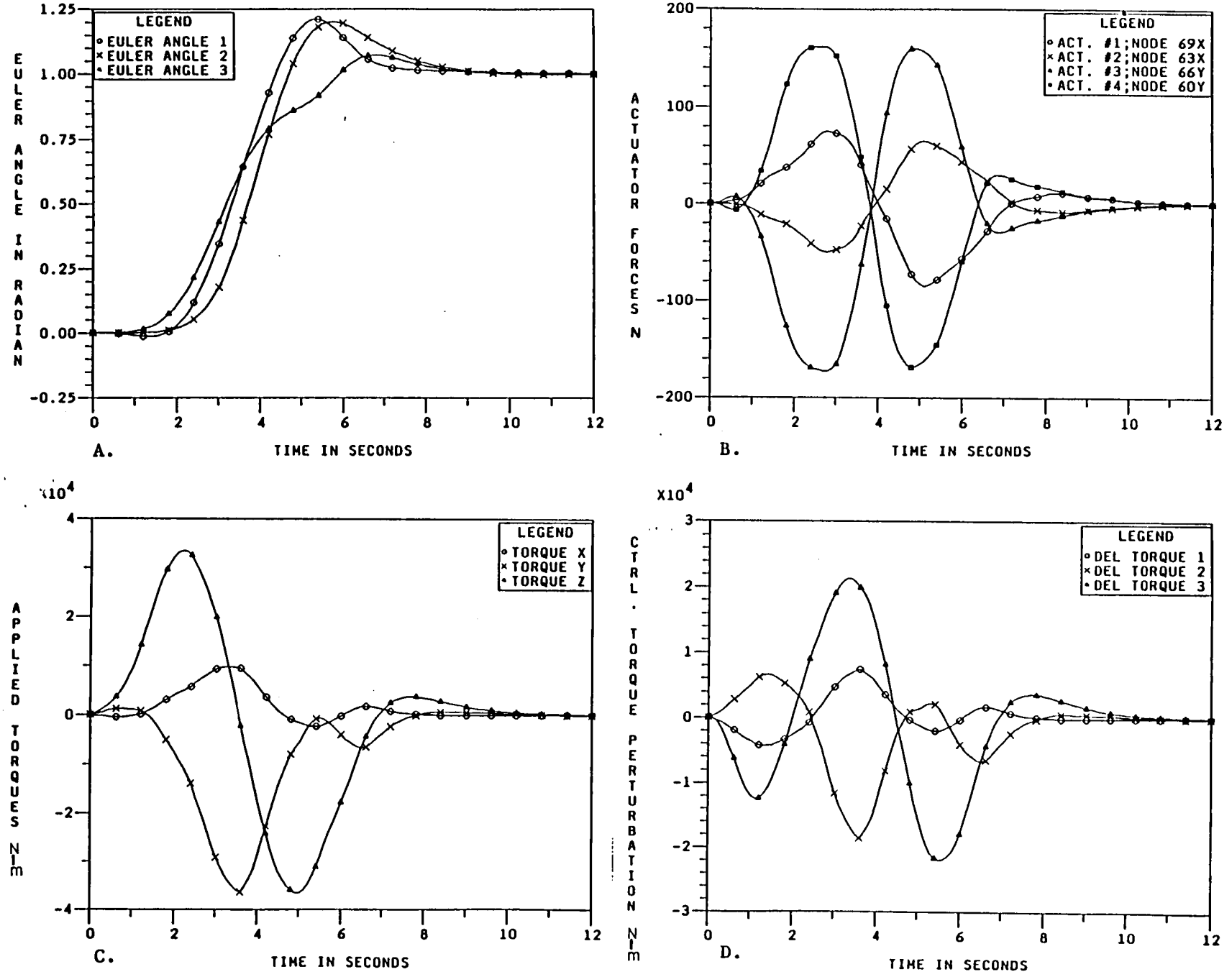

Figure 16. Feedback Control, 6 s Slew, Torquers + Force Actuators

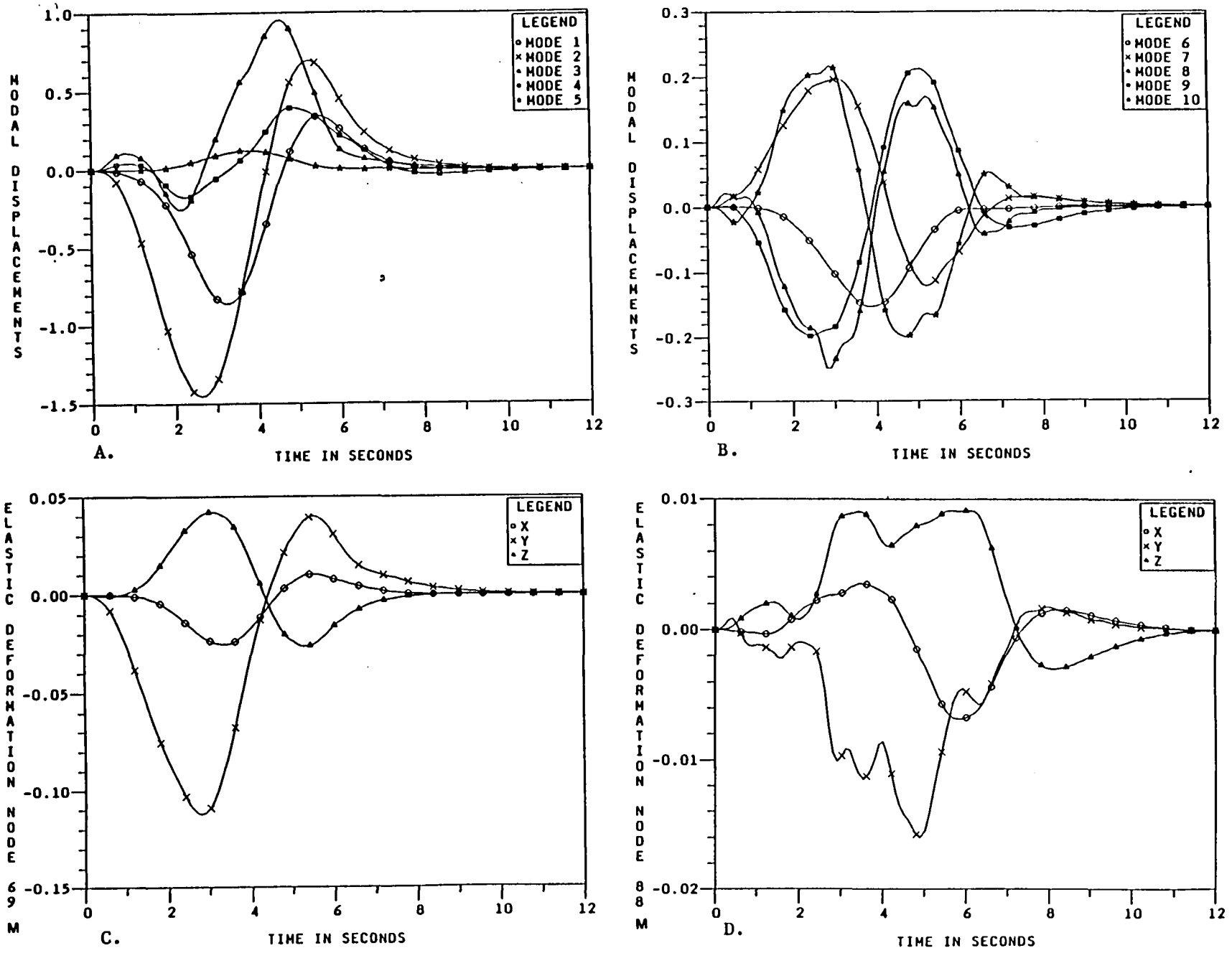

Figure 17. Feedback Control, 6 s Slew, Torquers + Force Actuators

selecting the weight matrices to produce comparable performance in both angular error and elastic deformation, the difference between torque-only control and torque-plus-force control is difficult to quantify. For the range of weighting matrices considered, it appears that the benefits of the additional force actuators are not significant.

In general, peak elastic deformations during the slew maneuver can be reduced by a factor of 2 when compared with the open-loop response. The typical reduction of the elastic deformation during the slew is about a factor of 4. The peak actuator force is about 70 N which could make the implementation of force actuators on the antennas rim difficult, if not impossible. However, one must keep in mind that the EPS structure is not designed for large rapid slews.

SLEW CONCLUSIONS AND RECOMMENDATIONS

Slew Conclusions

A DISCOS-based multibody simulation has been developed for the EPS model. The three-axis frequency-shaped slewing methodology of Chun, Turner, and Juang, 1987 has been implemented on this model. A baseline set of actuators has been defined for EPS involving torquers for the open-loop control, and a combination of torquers and force actuators for the perturbation feedback. Both 6 s and 10 s slew maneuvers have been designed for the EPS.

Results of the simulation test cases show that the combination of open-loop nominal profile, perturbation feedback, and disturbance feedforward performs well. The orientation errors and elastic deformations are reduced within a reasonable time after the end of the nominal maneuver time. All 10 s maneuver simulations meet the performance goal of 3% angular error and 10:1 reduction of open-loop deformations. The 6 s example maneuver requires a longer amount of time before the angular errors are reduced to that level; on the other hand, the elastic deformations are reduced by a factor of 100:1, which is an order of magnitude better than the design goal. An adjustment of the weight matrices could be made to improve the angular performance while keeping the elastic response within the 10:1 reduction goal.

The simulation results point out the difficulty of selecting proper weight matrices for achieving the desired response, particularly when there is a large number of states. For simplicity, the weight matrix selection has been limited to diagonal elements, even though is known that selection of non-zero off-diagonal elements allows greater mobility of the closed-loop poles. The use of off-diagonal weighting elements has not been considered for lack of time and appropriate software. It is anticipated that with an automated weight selection algorithm, all of the closed-loop responses can be tailored to the desired performance goals.

Slew Recommendations

In this study, the open-loop torques are provided by torque-generating devices at the CG of the structure. Future studies could consider the use of force actuators to provide part or all of the required torque. With suitable allocation of the force levels, this would reduce the amount of excitation to the elastic modes of the structure.

Actuator placement algorithms that account for the effects of the open-loop

torques should be used. Improvements to the perturbation feedback controller could include the constraining of perturbation forces so that they apply zero net torque to the structure and the development of a weight matrix selection algorithm to assist in controller design.

Robustness issues should be examined. These would include robustness to modeling errors in the structure and the actuators, and external noises.

A differential dynamic programming approach could be considered for producing a rigorously optimal solution to the open-loop finite-time rigid/flex maneuver problem as well as providing the optimal time-varying feedback gains for the perturbation controller. Time-varying gains could be fitted to Errors coefficients or other basis functions for use in gain scheduling.

This study demonstrates that the basic idea of open-loop nominal plus perturbation feedback is feasible. The choice of an LQR type of perturbation feedback is but one of many possible controller approaches. Future studies should consider different types of perturbation feedback controllers, depending on the mission requirements and computational capabilities.

INTEGRATED DESIGN: TECHNICAL AND SOFTWARE DEVELOPMENT ISSUES

Integrated design seeks to bring together several technical disciplines in a common work environment to model, analyze, predict performance, and optimize the controlled behavior of large flexible space systems. The analysis problem is multidisciplinary in nature. A complete investigation of the expected on-orbit performance of a mission concept can require a structural model, thermal model, disturbance model(s), control/estimation model, performance metric models, optical and/or radiometric models, dynamics models, ground test models and potentially other models. This process starts during the preliminary design phase for a new concept and continues throughout the life of a mission. Traditional spacecraft design approaches have developed approaches that have segregated activities along discipline lines. With the next generation of planned satellites there is an increasing need to closely coordinate the activities of different design groups in order to insure that the performance goals for the next generation of large lightweight joint-dominated systems can be achieved while reducing the mission risk to unanticipated design problems.

Design Issues for Large Space Structures

The design of Large Space Structures(LSS) is a multidisciplinary activity which embraces structures, structural dynamics, control, and multibody dynamics. The process starts with the identification of a new mission and the performance requirements required for achieving the science and engineering objectives. As science missions become more ambitious the spacecraft design community is forced to develop large systems in order to achieve the *sensitivity* and *resolution* requirements for analyzing the mission observables. An important byproduct of the need for large systems is that launch mass limits force the structural design towards lightweight low frequency structures. The performance tolerances tighten because larger systems have inherently greater resolving power. The resolving power of the instruments places constraints on the allowed levels of jitter motion for the structure. The characterization of the coupling effects between vehicle size and instrument performance is complicated because the effects are functionally dependent on the operational wavelength of the science instrument, the inherent resolving power of the device, the physical dimensions of the operational platform, and the signal processing capabilities available for analyzing the data. Large low-frequency systems can be shown to be highly susceptible to experiencing an induced response, and that the susceptibility increases nonlinearly with increasing vehicle size. Fortunately, heuristic criteria can be established that can be used as guidelines for determining when a new structural concept may require active control means for achieving the mission objectives. When an application has been identified where control is

required, then advanced technology can be beneficially applied and may in fact represent an enabling capability.

Genesis of the Interaction Problem

Mathematically, the need for active control arises when the bandwidths for the structural frequencies, the disturbances and the control are either close or overlapping (see Figure 18). When these bandwidths are close or overlapping a real possibility exists for exciting a resonant structural response which can either degrade the performance or damage the vehicle. The complexity of the control problem is assessed by evaluating the open-loop performance of the structure and determining whether any induced responses exceed the structural design performance specifications. When the response exceeds the design specifications then some form of control must be invoked in order to achieve acceptable system-level performance. There are four levels of control design complexity which characterize the difficulty of the problem, as listed in Table 1.

Table 1: CONTROL SYSTEM DESIGN COMPLEXITY

Problem Type	Performance Spec.* (Range)	Control Benefit
I	10^0-10^1	Enhancing Capability
II	10^1-10^4	Enabling Capability
III	10-10^6	Enabling Capability/ Multiple Technologies Required
IV	10≥10^6	Beyond the State-of-the-Art

* (Open-Loop Performance)/(Performance Goals)

Type I missions represent enhancing capabilities because many potential solution strategies are available, including: slight re-designs of the structure, added damping treatments, and system/component level isolation concepts.

Type II missions represent enabling capabilities because both classical and modern control approaches can be used to achieve the required levels of the system performance. As discussed in Turner, 1990, ACOSS-type control can be used for broadband disturbance inputs that induce open-loop responses exceeding the performance specifications in the range of [10^1, 10^2]. This capability is consistent with the goal of many ground-based experimental efforts, though to

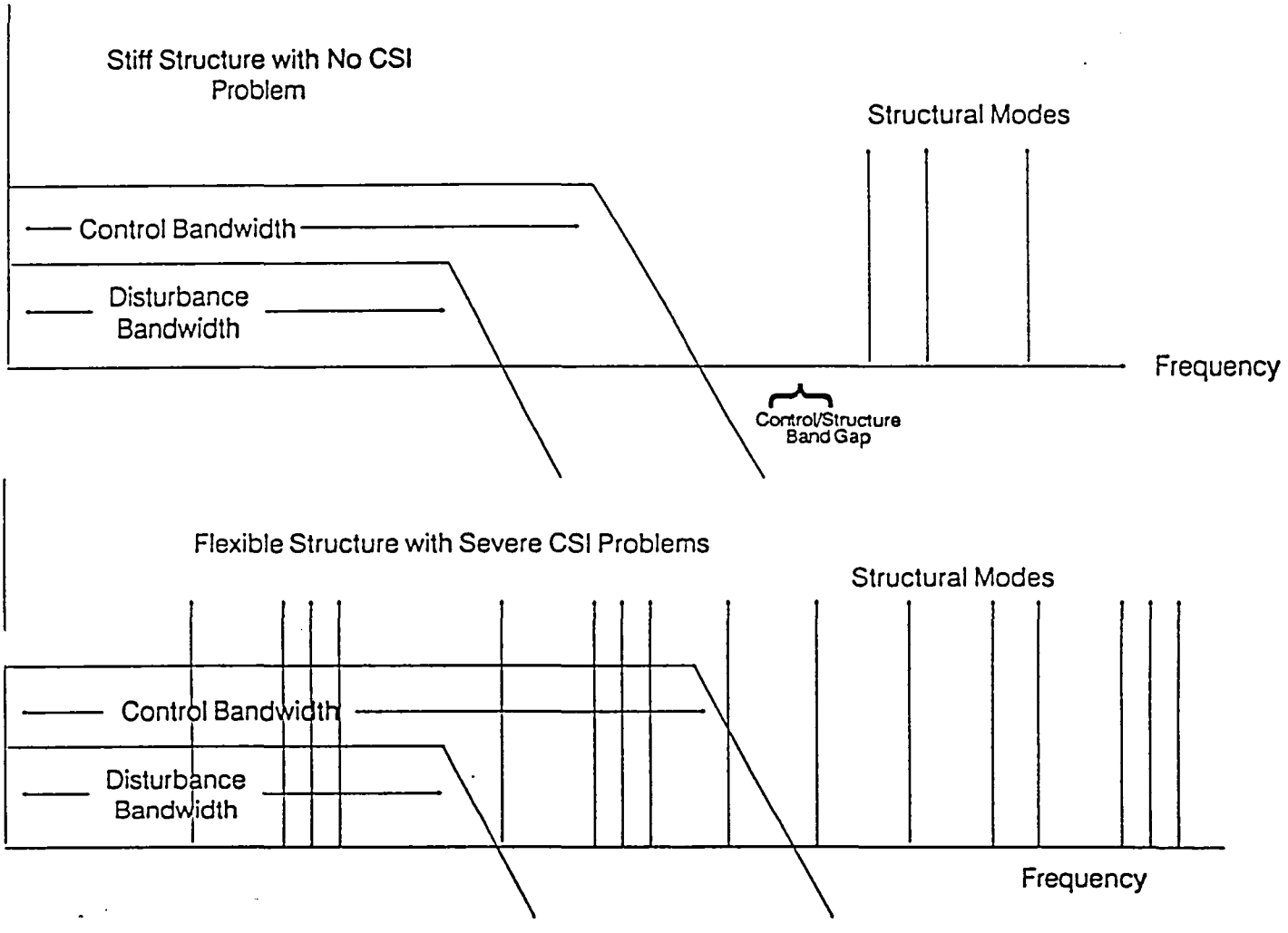

Figure 18. CSI Problem Complexity

date no results have been reported that corroborate the theoretical predictions throughout the performance range of interest. For response ratios in the range of $[10^2, 10^4]$ there are theoretical predictions which indicate that single-frequency disturbances can be suppressed using ACOSS technology.

Type III missions are enabling but require hierarchical approaches which combine passive damping treatments, active isolation concepts, broadband/single frequency modern control approaches, and optimization methodologies for obtaining a workable design.

Type IV missions are characterized by control requirements which exceed the state-of-the-art in one or more critical design technology areas.

Types II and *III* represent the applications where advanced design capabilities can be beneficially used for solving complex structures and control design problems. The technology issues which impact the development of an integrated analysis capability are presented in the following sections.

Control/Structure Interaction Technology

Control/Structure Interaction (CSI) technology provides a means for suppressing undesirable structural behaviors and achieving the mission objectives by either passive or active means. CSI is generally an enabling capability for systems which are either very large or subject to tight internal alignment constraints typical of optical systems.

In traditional spacecraft design approaches the structures and control teams have minimal levels of interaction during the design effort (see Figure 20). This approach works fine as long as the structure is basically rigid and the attitude and subsystem pointing controls and disturbances cannot induce a structural response. A key assumption of this approach is that small changes in either structural or control design will overcome any potential problems which may arise. As vehicles become larger, however, the need for coordination between design teams increases because many potential problems can be easily fixed during the early phases of a project. On the other hand, if the problems are only uncovered late in a project, the impact on time and cost can be significant. Moreover, failure to detect CSI related design flaws can lead to either greatly degraded system performance or catastrophic system failure.

A fully integrated analysis approach can offer a number of distinct advantages for a spacecraft design group. The key objectives and payoffs which result form an integrated software design effort.

Technical Issues	Potential Concerns	Resolution/Tradeoff
Modeling Accuracy	•Nonlinear Effects •Fluid Motion •Stability •Performance	•Material Nonlinear Joint Fluid Motion Models Increased Fidelity vs. Computational Cost •Ground Testing •System ID, Adaptive Control
Control Law Design	•ROM Spillover •Robustness •Performance	•Improved Model Selection/ROM •Robust Design Techniques •Nonconservative Analysis Techniques •Distributed Control Approaches •Adaptive Control
Sensors & Actuators	•Poor Performance Due to Bandwidth, Saturation, Resolution, Noise, Nonlinearity, Placement •Failures	•New Technology (Fiber Optics, Electro-Optics, Piezoelectrics) •Optimal Placement Methods •Testing and Refinement •Redundancy Management
System Identification	•Resolution of Closely Spaced Modes •Computational Complexity •Sensor Resolution and Bandwidth •Nonlinearities	•Stochastic Methods •Adaptive Methods •Parallel Processing
System Validation	•Testing in 1-G •Facilities for LSS •Suspension & Scaling •Cost	•Develop Space-Validated Analytical Tools •Novel, Active 0-G Suspension •Scaling Laws •New Facilities

Figure 19. Key CSI Technical Issues

Objectives

- Automated tool for preliminary and advanced structural and control design
- Emphasis on multidisciplinary aspects of the design task

Payoffs

- Improved design team communication
- Enhanced designs
- Testbed for evaluating emerging analytical design methodologies
- Reduce CSI risks

The structural behavior is measured relative to the mission performance goals. To measure the system performance a model is developed which consists of a normal mode model (e.g., typically obtained from a *finite element model*) and a disturbance model which consists of both on-board and environmental mechanical loads. By simulating the performance of the system without CSI control technology the complexity of the problem can be assessed. For example, if the line-of-sight pointing error and jitter exceed the allowed tolerances for achieving the science and engineering goals, several options are available for carrying out corrective action, including:

- Structural Redesign
- Advanced Materials/Damping Treatments
- System/Component Isolation Concepts
- Vibration Control
  - -Shape Control
  - -Figure Control
  - -Slew Control
  - -Vibration Suppression

An integrated design environment provides an opportunity for evaluating new and emerging control design approaches in a standardized evaluation context. This approach is ideal for minimizing the time required for transferring new technology development efforts from the research community to the spacecraft design community.

The key technical issues which affect the complexity of CSI design efforts are listed as follows:

Modeling Accuracy

Control Law Design
Sensors and Actuators
System Identification
System Validation

Each of these issues is complicated because of explicit and implicit coupling effects that arise through modeling idealizations and approximations, algorithmic limitations, as well as hardware limitations and manufacturing errors (see Figure 19).

CSI Technical Issues: Modeling Accuracy

Modeling accuracy defines how well the physical parameters describing the structural model are known. These parameters can include: geometry, mass distribution, stiffness distribution, frequencies, mode shapes, joint behavior, control system dynamics, and disturbance dynamics. This issue is important because errors in the mathematical model directly impact the stability, robustness, and performance characteristics of the control design effort. When modern multi-input and multi-output control approaches are invoked it is well-known that high levels of system performance can only be maintained when both the model for the structure and the estimated structural behaviors are accurate. An early and very important step in the model development process consists of selecting a suitable reduced-order model from the finite element description of the structural behavior. This step is important because it involves trade-offs between model fidelity, computational complexity, system performance and stability. Several of the currently popular reduced-order model selection methodologies are presented as follows:

Gain Factor Analysis
Singular Value Decomposition
Internal Balancing
Modal Cost Analysis
Chained Aggregation

A discussion of these techniques can be found in Turner, 1990.

CSI Technical Issues: Control Law Design

A control law design is basically a mathematical process whereby a strategy is developed for using estimates for the instantaneous system state to correct errors in the system performance. Either classical or modern control approaches can be used. However, only the modern control approaches have the theoretical

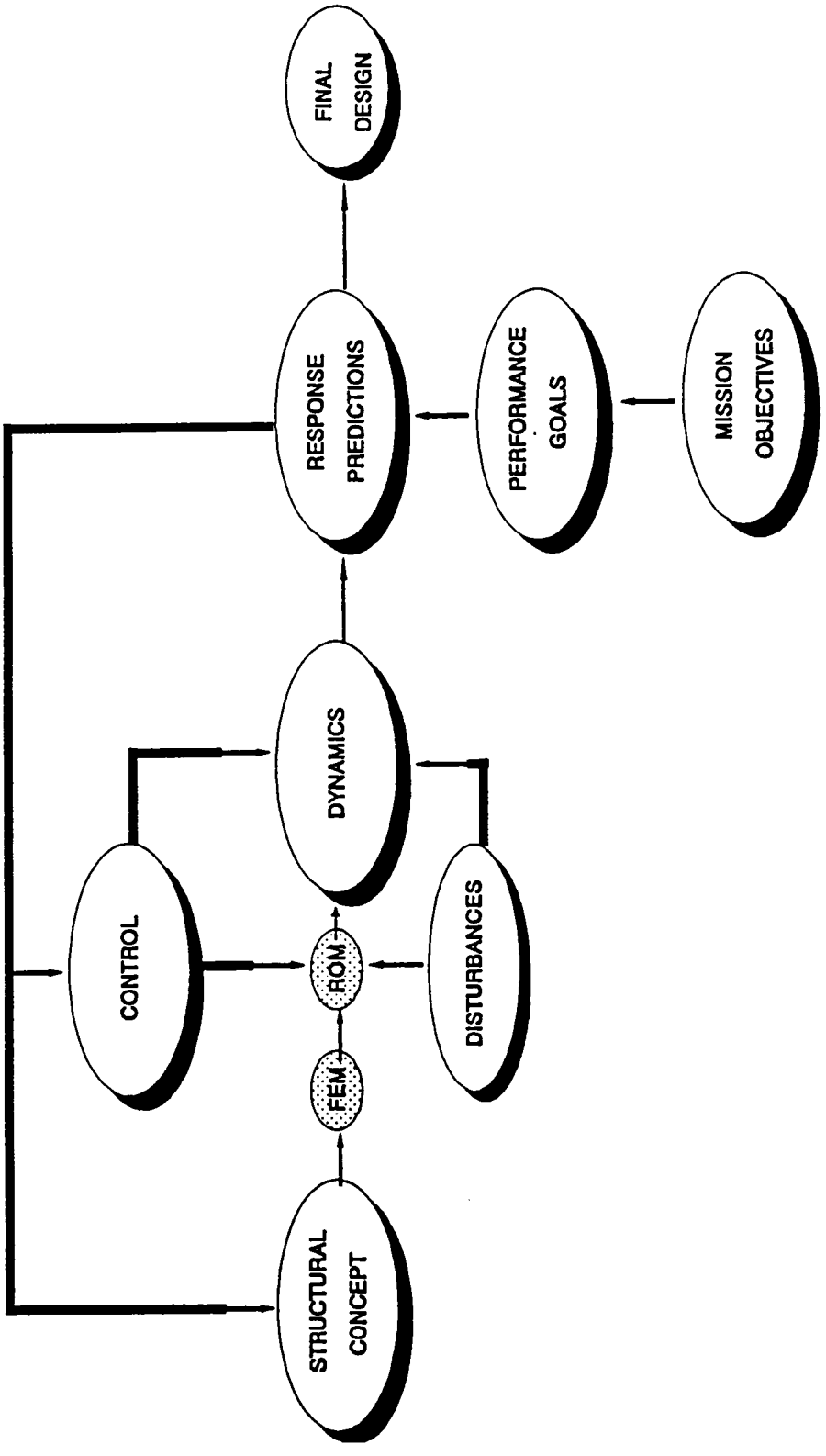

Figure 20. Conventional System Design Flow Diagram

capability for handling multiple inputs and outputs simultaneously. A partial listing of the currently available control design methodologies are presented in what follows:

Direct Output Feedback
Parameter Optimization
Orthogonal Filter
Positivity/Characteristic Gain
High Authority/Low Authority Control
Model Error Sensitivity Suppression
LQG/LTR
H^{∞}, H^{2}, L^{∞}
Maximum Entropy
Adaptive Methods

These methods are discussed in Turner, 1990.

CSI Technical Issues: Sensors and Actuators

Sensors are used to obtain measurements of the system state that can consist of translational and rotational position and velocity data. The actuators provide the means for carrying out force and torque commands for achieving closed-loop control objectives. The limiting factors which affect the accuracy of these devices are bandwidth, resolution, biases and scale factors for the inputs and outputs. These components act as the ultimate constraints on the achievable performance for any system.

CSI Technical Issues: System Identification

Because any control system design is based on various modeling assumptions a high performance control system can only be expected to operate successfully when the model parameters are well-known. The approach used for determining the model parameters form observations of the system response is system identification. Through analysis, system identification refines parameter estimates so as to make the model predictions more closely agree with the observed behavior. This technology becomes particularly important as the performance specifications tighten the limits on the allowed motions, thereby forcing the control system to perform extremely accurate feedback commands. Several of the currently available algorithms for carrying out the system identification function are listed as follows (Turner, 1990):

Cross-Correlation
Transfer Functions
Kalman-Filtering
Lattice Filter
ERA
Maximum Likelihood Method
ITD

CSI Technical Issues: System Validation

Both ground- and space-based system validations are required in order to ensure that the performance specifications are achieved and that the system is stable when operating in the presence of realistic disturbance sources. Tests of the actual operational hardware provides the only reliable methods for assessing the behavior of complex systems. The tests also provide ideal opportunities for validating analysis tools and improving one's understanding of the modeling process. When system structural concepts become too large to experimentally validate on the ground, one is forced to depend exclusively on analysis tools. For this class of applications there is a clear need for developing, testing, and validating software analysis tools.

INTEGRATED DESIGN APPROACH

Integrated design implies that the needs of several technology areas are considered simultaneously. For example, when the needs of structures and control are considered, one can seek a minimum weight structure where the control/estimation/system identification gains are determined subject to constraints on allowed subsystem motions, closed-loop pole locations, and numbers of sensors and actuators. For an integrated design approach to be effective the desired engineering approach consists of having all computational tasks carried out in a common simulation environment (see Figure 21). This approach ensures the consistency of data links from the structures design, control design, thermal design, optics/radiometric design, multibody models, optimization , and system-level evaluations. An integrated design strategy seeks to exploit a team approach for addressing design problems, thereby minimizing the traditional institutional barriers which act to segregate design group members along discipline lines.

Review of Research in Integrated Design

Integrated design during the last eight years has been used to refer to simultaneous or dual optimization studies where the design variables have consisted of both structural and control parameters. A major goal of an integrated design effort is to determine a better design for vehicles, where the success of a design is measured by evaluating performance measures such as minimum time, minimum fuel, minimum control effort, minimum weight, and minimum cost.

Mathematical optimization approaches are used for successively refining the structure and control designs, because of the multidimensional nature of the problem. A generic description of the mathematical statement of an optimization problem is presented in the following section.

Generalized Kuhn-Tucker Conditions

An optimization problem is defined by specifying the free variables which can be adjusted in a successive approximation algorithm that seeks to improve some measure of the system performance. To ensure that a physically meaningful set of design variables results from the optimization process one must specify constraints. For example, cross sectional beam areas must always be positive real numbers. The searching algorithms are provided measures of the system performance, such a quadratic performance indices which penalize structural response and control effort. By measuring the sensitivity of the performance

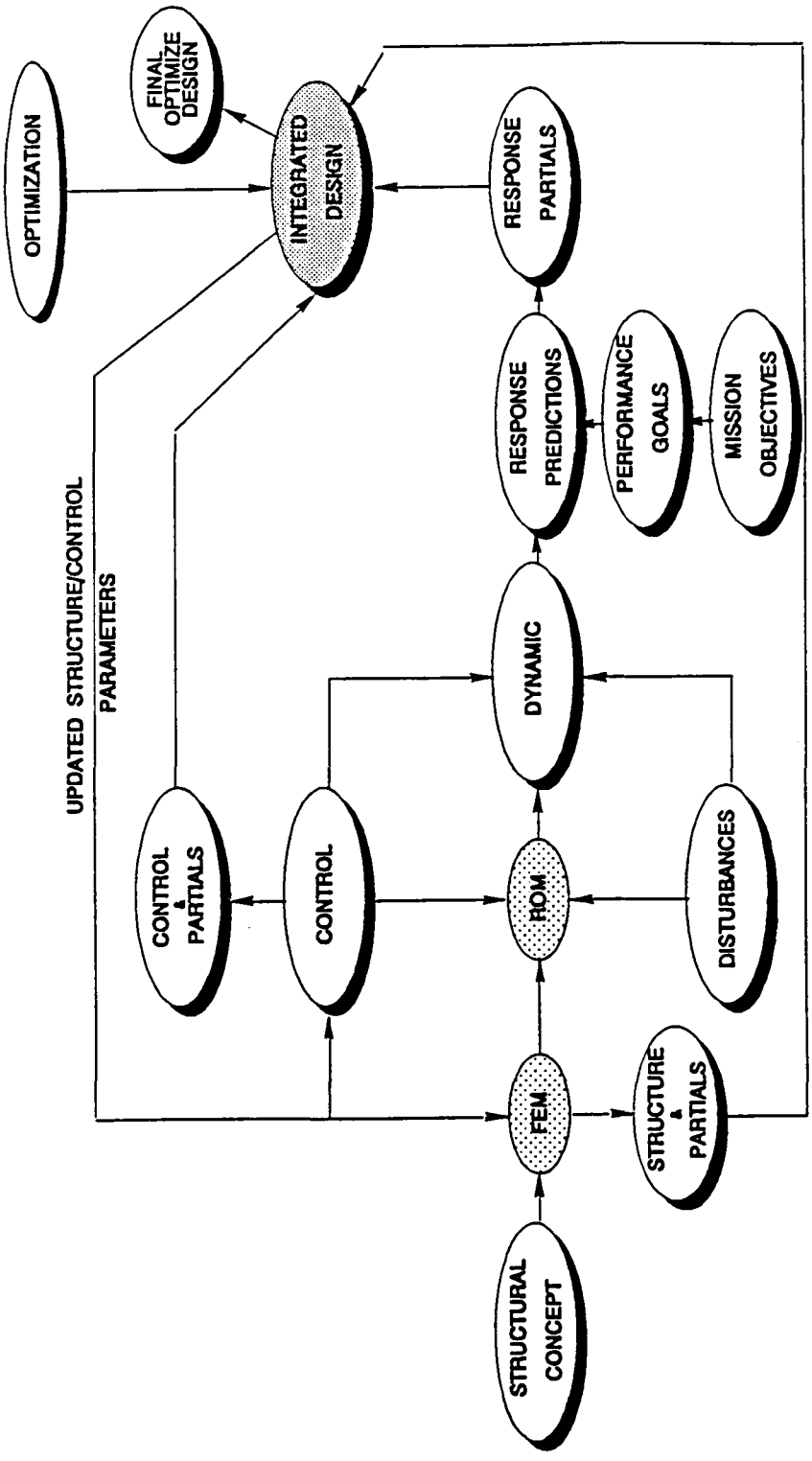

Figure 21. Integrated Design Flow Diagram

measures, one can define incremental changes in the design variables that minimize (maximize) the performance measures locally. Mathematically the optimization process can be described as follows:

Find D_i, $i = 1, \ldots, n$, such that (D_i ▲ Design Variable)

Minimize (Maximize) $F(D_1, \ldots, D_n)$ (Scalar or Vector)

Subject to the Constraints

$h_j(D_1, \ldots, D_n) = 0$, $j = 1, \ldots, p$ (Equality Constraints)

$g_k(D_1, \ldots, D_n) \geq 0$, $k = 1, \ldots, q$ (Inequality Constraints)

Form the Augmented Objective Function

$$\mathcal{F} = F(D_1, \ldots, D_n) + \sum_{j=1}^{p} \lambda_j h_j(D_1, \ldots, D_n) + \sum_{k=1}^{q} \mu_k [g_k(D_1, \ldots, D_n) + S_k^2] \qquad (38)$$

where

λ_j Denotes the Equality Constraint Lagrange Multiplier

μ_k Denotes the Inequality Constraint Lagrange Multiplier

S_k^2 Denotes the Inequality Constraint Slack Variable

The necessary conditions which define the mathematical requirements for determining an optimal solution are:

$$\partial F/\partial D_i + \sum_{j=1}^{p} \lambda_j \partial h_j/\partial D_i + \sum_{k=1}^{q} \mu_k \partial g_k/\partial D_i = 0, \ (i = 1, \ldots, n)$$

where

$\mu_k = 0$ if $g_k(*) > 0$ and $\mu_k \geq 0$ if $g_k = 0$

The basic mathematical problem statement is highly nonlinear and successive approximation strategies provide the only rational approach for systematically refining estimates for the optimal set of design variables. Numerical optimization problems are difficult for two reasons. First, initial starting guesses must be specified which must satisfy the constraint conditions for the algorithm to start with a feasible solution. Second, the analyst must be constantly alert to the possibility that multiple minima (maxima) can attract the optimization algorithms, leading to converged solutions that may not be globally

optimal.

Optimization based design techniques have been developed for many years (Crane, Hillstrom and Minkoff, 1980; Arora, Thanedar and Tseng, 1985; Grandhi, Thareja and Haftka, 1985; Gill, Hammarling, Murray, and Wright, 1986; Gill, Murray, Saunders and Wright, 1986; Gill, Murray and Wright, 1981; Polak, Siegel, Wuu, Nye and Mayne, 1985; Palacios-Gomez, 1980; Vanderplaats, 1973; Goldfarb, 1969; Venkayya and Tischler, 1978, 1979). At this time there are several commercially available tools which have implemented several of the multidimensional search algorithms. They include:

Recursive Quadratic Programming
Homotopy-Based Optimization Methods
Gradient Projection
Reduced Gradient Methods
Feasible Directions Methods
Optimality Criteria Methods
Sequential Linear Programming Methods
Projection Methods
Sequential Unconstrained Minimization Techniques
Multiplier Methods (Augmented Lagrangian)

The usefulness of any of these methods depends on the special features of the problem at hand. Some of the methods make exclusive use of first-order sensitivity data, others either compute exact expressions for the second-order sensitivity data or approximate this information by various algorithmic strategies (Heylen, 1986; Rudisill, 1974; Fox and Kapoor, 1968; Plaut and Huseyin, 1973; Haug and Rousselet, 1980a,b). Common to each of the methods is the need for defining measures or performance indices for measuring the effectiveness of parameter refinement strategies, evaluating any constraints which limit the allowed range of acceptable solutions, computing the sensitivity of the performance measures and the active constraint sets to variations in the current estimates for the design variables.

The calculation of the sensitivity data represents a computationally intensive part of any optimization-based study. There are two frequently used methods for generating the required partials: finite difference techniques and analytic partials. The finite difference technique is conceptually the simplest approach because one uses numerical perturbation techniques to generate approximations for the required partial derivatives (Rudisill, 1974; Cronin, 1988; Mills-Curran, Lust and Schmit, 1983; Lust and Schmit, 1986; Fox and Kapoor, 1968; Prasad, 1984; Fleury and Schmit, 1980; Palacios-Gomez, 1980; Vanderplaats,

1984; Goldfarb, 1969; Plaut and Huseyin, 1973). A potential disadvantage of the finite difference technique is that the numerical procedure can be iterative and expensive if the model itself is computationally intensive to evaluate. The analytic partials approach assumes that closed-form expressions can be developed which can be used to provide the sensitivity to machine precision. When practical the analytic partials approach is preferred because all the data can be generated with a singe operation.

Optimization for Structural Applications

There is an extensive literature which describes application of optimization-based methodologies for structural applications (Fraser, 1985; Grandhi, Thareja and Haftka, 1985; Choi, Haug and Seong, 1983; Zeischsha, Leuridan, Storrer and Vandeurzen, 1988; Heylen, 1986; Cronin, 1988; Hou and Twu, 1986; Woo, 1987; Khan, Thornton and Willmert, 1982; Yoshida and Vanderplaats, 1985; Rubin, 1970; Fleury and Schmit, 1980; Pedersen, 1982; Shiau and Chang, 1988; Kamat, Venkayya and Khot, 1983; Khot, 1985; Grandhi and Venkayya, 1987; Shin, Plaut and Haftka, 1987; Thareja and Haftka, 1986; Canfield, Grandhi and Venkayya, 1986; Venkayya and Tischler, 1978). Typical design approaches define performance measure(s) and constraints (geometrical-manufacturing limits, practicality, behavioral-pole placement, peak deflections). Typical structural performance indices include:

Cost
Weight
Stress
Stiffness
Deflection
Frequency
Mode Shape
Fatigue Life
Reliability

Many times it may be necessary to consider several performance indices simultaneously in order to obtain a practical design. A standard approach is to consider a linear combination of performance indices that are multiplied by weighting coefficients which are assigned based on some heuristic criteria. This approach is capable of producing numerical results that satisfy the necessary conditions for the optimal solution. Nevertheless, there are many tradeoffs between the different objectives that can not be fully investigated via this approach. The alternative to the scalarization of several performance indices is to consider vector performance indices. This approach, however, has received

little attention in the technical community.

Typical structural design variables for an optimization process include:

- Cross-sectional areas
- Thickness
- Inertial & Torsional Properties
- Topological (Members & Joints)
  - -Number
  - -Sequence
  - -Connectivity
- Geometrical (Coordinates of Joints)
  - -x,y,z,ϕ,θ,ψ
- Shape
  - -Cross-Sectional
  - -Boundary
- Material
  - -Fiber Orientation
  - -Passive Damping Distribution
- Loading
  - -Location
  - -Number
  - -Type of Support
  - -External Loads

Optimization for Control Applications

In any control scheme there are free parameters which can be adjusted in order to achieve desired levels of system performance. Indeed, in modern control approaches the necessary conditions for the state and costate differential equations require that the elements of several matrices be specified, leading to a parameter optimization problem at the very start of the problem. Because the necessary conditions for an optimal control solution are naturally described by coupled systems of nonlinear differential equations, where the known boundary conditions are split between the initial time and final time, many first- and second-order optimization methods have been developed for solving these problems. The trajectory control problems are typically open-loop control problems, though several second-order methods also produce time-varying feedback gains. The use of optimization-based methods has been a natural part of the solution process for

control problems that have been defined by integral-variational formulations. (Boyd, Balakrishnan, Barrat, Khraishi, Li, Meyer and Norman, 1988; Desoer and Gustafson, 1984; Doyle, 1982; Doyle and Stein, 1981; Francis and Zames, 1984; Ly, Bryson and Cannon, 1983; Polak, Siegel, Wuu, Nye and Mayne, 1985; Safonov, 1986; Garibotti, 1984; Walsh, 1987; Manning and Schmit, (1987).

Many performance measures can serve to define optimal control problems. One of the great benefits of numerical optimization methodologies is that classical design criteria can be combined with modern multi-input/multi-output designs in a systematic way. As in the case of structural when scaler combinations of different objectives are combined many potential options are lost. Alternatively, vector objective functions may be the best approach for dealing with conflicting design objectives. Typical control performance goals measures and technologies are listed as follows:

- Pole locations
  - -Control Gains
  - -Estimator Gains
- Performance Index(es)
- Control Type
  - -Regulator
  - -Tracking
  - -Disturbance Accommodation
  - -Frequency Shaping
  - -Differential Dynamic Programming
- Controllability
- Observability
- Robustness
- Transfer Function Behavior
- Loop Stability
- Frequency-Domain Loop Shaping
- Design Criteria
  - -Stability Margins
  - -Bandwidth
  - -Damping
  - -Overshoot

The design variables for the control design can include both algorithm related parameters and hardware design and placement issues. Typical control design variables are listed as follows:

- Sensor/Actuator Placement
- Weight Matrices

  -State
  -Control
  -Terminal Penalties
  -Estimator
  -Feedback/Feedforward Gains

Optimization for Integrated Design Applications

The application of optimization-based techniques for simultaneous structure and control design began with the work of Hale, Lisowski and Dahl, 1982, in which they considered a single-axis slewing control problem for a flexible structure. The basic structure consisted of a central hub with four symmetrically attached elastic appendages. They considered the problem of minimizing a quadratic performance index. Their control formulation consisted of an open-loop maneuver profile. The design variables for the structure consisted of the boom taper and the design variable for the control consisted of the state and control weighting matrices. The coupling between the control and structural problems arises through the closed-form expression which is obtained for the performance index, because the performance index is minimized subject to the equations of motion as a differential equation constraint. A gradient projection algorithm is used to refine the approximations for the design variables. This work stimulated many additional investigations into the area of integrated design methodology. A brief summary of other related work is presented in Table 2. The authors listed in Table 2 represent the individuals who have made significant and innovative contributions to the literature.

Table 2. RESEARCH IN INTEGRATED DESIGN

Author(s)	Problem Description
Salama, Hamidi and Demsetz, 1984	Feedback Control, LQG, Second-Order Newton-Raphson Iteration, Steady-State Riccati Equation
Messac and Turner, 1984	LQG, Steady-State and Finite-Time Control, Single-Axis Slew Control, Minimum Weight Structure
Haftka, Martinovic and Hallauer, 1985	Grillage Control, Steady-State and Control, Simplified Structural Changes for Control, Theory and Experiment
Junkins, Bodden and Turner, 1984	Generalized Quadratic Performance Index, Slewing, Homotopy Minimum Norm Optimization
Miller and Shim, 1986	Truss Structure, Gradient Search, Steady-State
Khot, Grandhi and Venkayya, 1986-present	Steady-State Control, Minimum Weight, Gain Norm Constraints
Adamian and Gibson, 1986	LQG, Minimum Weight, Control Robustness, ADS Optimization
Cooper, Young and Sutter, 1986	IMAT Based Structure/Control Design
Kyong and Junkins, 1988	Open-Loop, LQG, Sensors and Actuator Placement, Homotopy/ Simplex Optimization
Lust and Schmit, 1988	Direct Output Feedback, CONMIN
Gustafson, Aswani, Doran and Tseng, 1985	Continuum and Frequency Domain Design Techniques
Miller and Shim, 1986	Minimum Weight and Minimum Control Energy, Gradient Optimization
Belvin and Park, 1988 & 1990	LQG, ADS Optimization, LASS, ORACLS, CS^3 Prototype System
Onoda and Hafka, 1987	Minimum Weight and Cost Minimization

There are two classes of spacecraft operational conditions which require different control approaches. First, finite time transient problems which are typical of slewing control problems. These problems are not likely to induce a resonant response in the structural behavior because the slew disturbance stops at the end of the maneuver. Second, infinite time problems which correspond to steady-state vehicle operations where a persistent disturbance source(s) acts to induce a structural response which must be suppressed by active means. The issues of control system stability and robustness are more critical for problems of the this type. Most of the research activity listed in Table 2 has been focused on the finite time slewing control class of optimization problems. To date there have been no realistic infinite time problems and solution approaches discussed in the technical literature. This issue is important because the majority of real spacecraft applications can be expected to be of infinite time variety, hence, a need remains for exploring the computational and algorithmic issues associated with this class of technical problems.

Several general conclusions can be reached regarding the research conducted to date on the problem of integrated design. First, this work has demonstrated the basic feasibility for conducting fully integrated design efforts. Second, much of the effort of the individual researchers has focused on obtaining the analytic partial derivatives required for the optimization algorithms. This information has been widely disseminated in the literature but no general-purpose capabilities exist at any one organization. In problems where researchers have used approximate finite difference techniques to compute the sensitivity partial derivatives it has been consistently reported that the structural partial derivative calculations dominate the computer run times. As a result, this observation has stimulated much work in the area of developing analytic partials for the structural models, using typical eigenvalue/eigenvector data obtained from finite element programs such as NASTRAN. Third, there has been no community-wide convergence to a best method for attacking this class of problems, though several methods appear to work equally well. Fourth, no large-order problems have been exercised to date (i.e., less than 100 degrees of freedom). Fifth, some simplified approaches have been presented and appear to be useful for limited classes of problems. Sixth, no theoretical obstacles have been encountered which can limit the extension of existing results to problems of arbitrary complexity.

Integrated Analysis Software Design Capability

The development of an integrated analysis capability must first identify the expected user group for the tool in order to ensure that the flexibility and generality required in an operational spacecraft design environment is properly

developed. As presented in Figure 22 there are three levels of user groups which can be expected to interface with an integrated design tool. First, *system engineers* whose basic interest is in conducting system-level performance assessments and trade studies, particularly during preliminary design studies. To support these users the integration software capabilities across all technical disciplines is an absolute requirement. Here algorithm robustness is more critical than efficiency because these engineers will generally be interested in low-dimensioned problems. These users would not be expected to understand the technical underpinnings of all of the software packages they must use. As a result, the integrated analysis capability must be design to function as a black box for these users, because they would never be expected to modify the core analysis software in any way. Second, *discipline specialists* whose primary interest would be in conducting detailed trade studies in an individual technical area. Here only a medium-level of problem integration is required across the supporting technical disciplines. This class of users would be expected to conduct stressing performance assessments with high-fidelity/high-dimensioned problems in their technical areas of interest. These users would not be expected to modify the core analysis software in order to carry out their studies. Third, *basic researchers* whose major goal is the develop and testing of advanced capabilities in their technical disciplines. Here only a low-level of problem integration is required across the supporting technical disciplines. Typical problems can be expected to be of high dimension and representing state-of-the-art capabilities. These users would be expected to integrate their software developments within the integrated design capability. Clearly the needs of the potential user groups are very different but they can all be addressed within a common framework.

- LEVEL 1: SYSTEM ENGINEERING
- LEVEL 2: DISCIPLINE SPECIALISTS
- LEVEL 3: RESeARCHERS

n65

Figure 22. Multi-Level Functionality User Groups for an Integrated Design

PROGRAM PLAN FOR DEVELOPING AN INTEGRATED DESIGN TOOL

Development Options

There are three development options which should be considered for building an integrated design tool. First, one could expand on the multidisciplinary optimization efforts that have been under development by either Sobieski, 1982, 1984; or Venkkaya, 1978, 1979, 1987. This approach would ensure technical impeccability of the analysis tools. Unfortunately, these tools have been designed for use by researchers in the field of optimization and would therefore be difficult for generalists to use. Second, one could seek to build the capability from scratch, however. This approach is potentially too costly and does not leverage the previous significant government investments in analysis capabilities. Third, one can build on existing multidisciplinary tools such as IMAT(LaRC), IAC(GSFC), and ISM(AFWL). IMAT exists at LaRC and provides connections for structures and control through a common data base design. IAC provides a general architecture for connecting many analysis capabilities but represents a precursor to ISM. ISM has the most promise but is currently beginning pre-beta testing and will not be available for some time. As a result, for the near term the best approach is to build a prototype capability based on in-house tools available at LaRC. Over time the supporting capabilities developed for the prototype tool could be transferred to ISM for building the general-purpose tool. Figure 23 presents a potential structure for a long-term integrated design development effort. The basic tool would have an interface which accesses ISM. ISM would act as a database manager for controlling the internal flow of information between the different technology computational modules. The key point to observe is that the optimization, control, structures, thermal, optics, radar, and associated sensitivity partial derivatives all share common databases, workspace, host files, system utilities, and compiler optimization. Through the user interface/executive system, users can control the level of integration across the available discipline tools and the level of complexity required within individual technology areas. The identification of the multiple levels of users needs ensures that a broad base of engineers and scientists can fully exploit the unique capabilities that such a tool can provide.

A proposed approach for developing the prototpye capability follows.

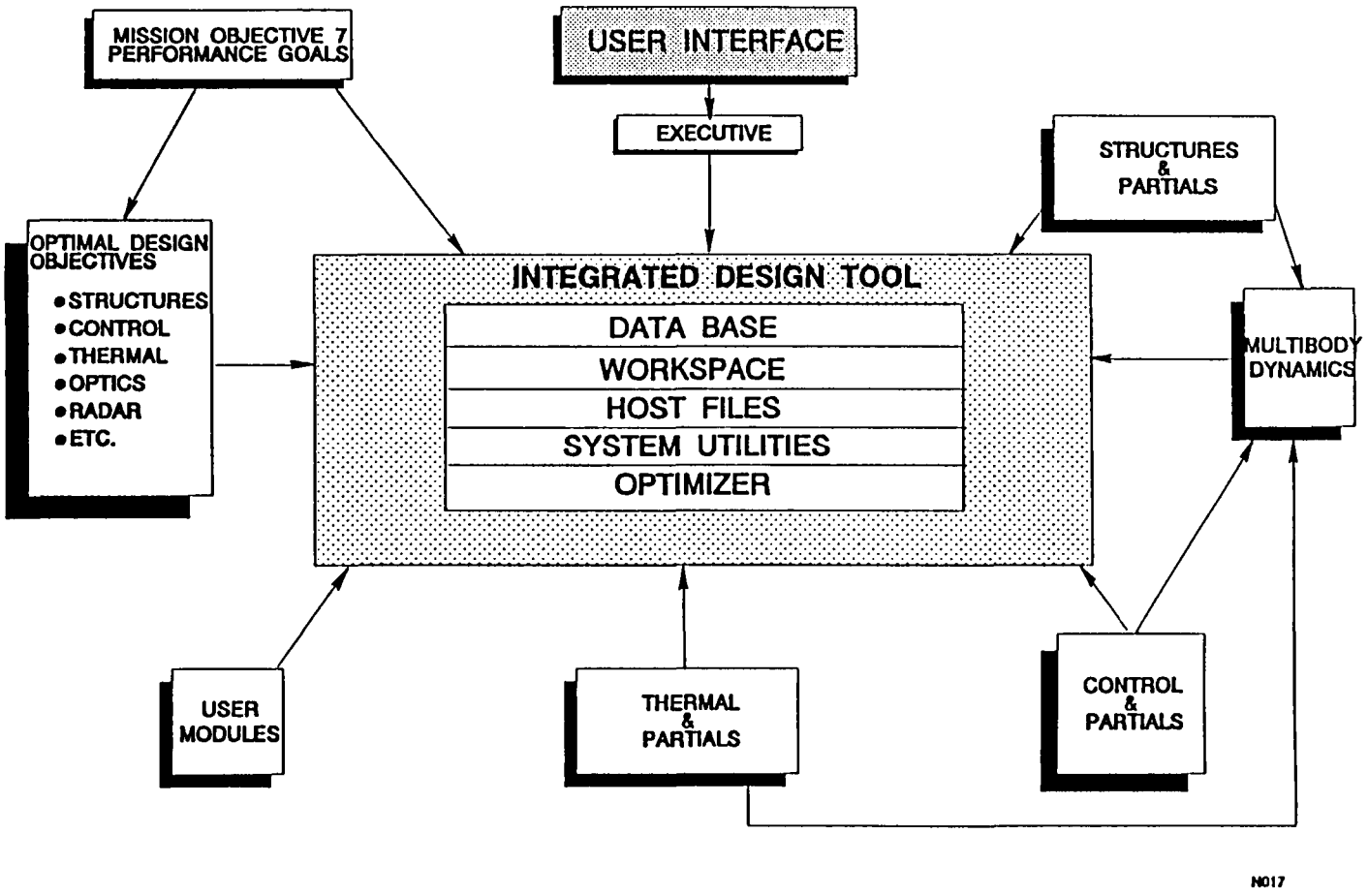

Figure 23. Structure of an Integrated Design Tool

Prototype Integrated Design Capability

There are several early design considerations which must be taken into account. These include:

- Modular Design
  - -To Readily Accommodate New/Improved Tools
- Interfaces to Existing Design Tools
  - -IAC
  - -ISM
  - -ASTROS
  - -MATRIXx
  - -ADS
- Development of an Application Library
  - -Standardized Test Problems & Results
  - -Archive Demonstrated SOA Capabilities
- Planning for Parallel Research & Hardware Validation Efforts
  - -Structures
  - -Control
  - -Optimization
  - -Algorithm Development
  - -Parallel Computational Architectures
- Target Computer Platforms
  - -High Performance 386 & 486 PC's
  - -Workstations
  - -Mainframes
  - -Parallel Machines
  - -Supercomputers

Beyond these top-level design considerations the specific ingredients of a prototype integrated design tool must be defined. To make full use of LaRC's existing capabilities, the following approach is proposed for developing a near-term in-house prototype capability:

- Use IMAT as the Core Database Manager
  - -MSC/NASTRAN (Structures Finite Element Code)
  - -MATRIXx (Classical & Modern Control Design Code)
- Use ADS as the Optimization Tool
  - -Industry Standard Software
- Develop Finite Difference Methodologies for Partials
  - -Provides Near-Term Operational Capability
- Develop Analytical Partial Models for Specified Controls and Structures Applications

-Implement LQG and Pole Placement Control Algorithms
-Develop Library of Analytical Partials for Future Applications

- Develop the Prototype Program Executive
- Validate the Prototype Tool by Analyzing Previously Published Applications
- Develop Ground Test Article for Designing, Testing, and Validating the Predictions of the Integrated Design Tool

The architecture for the proposed system is presented in Figure 24. The basic idea is to use the existing in-house capability to the greatest extent possible. This approach combines the structural analysis, control synthesis, and response predictions that exist through IMAT. The new software to be developed will consist of the integrated design interface/executive, ADS, structural partials, control partials, and response partials, where the partials are calculated initially via finite difference approaches. Under model development it is recommended that standard application problems such as the Draper/RPL model, planar truss, Class II, and Class IV models be developed. The Class IV problems will represent a stressing state-of-the-art application which will require that IMAT be modified to run a multibody program such as DISCOS in order to generate the platform and robot manipulator trajectory dynamics and loads.

Tasks and Resources Required to Develop Prototype Tool

Figure 25 presents a 24-month program for developing an in-house LaRC prototype integrated design capability. The first year builds and tests the basic connections between software tools and implements several classical and modern control approaches. Preliminary integrated design results will be available at the end of the first year assuming that the DARPA/RPL model is used. A task is also identified for planning the transition from the prototype tool to an ISM-based capability in the future. This future capability will be fully capable of analyzing and designing any foreseeable system that NASA can envision in the next ten to twenty years. Manpower estimates are also provided for carrying out the individual tasks. The entire prototype development effort is estimated to require approximately four man-years to complete.

Figure 24 Prototype Software Development Plan

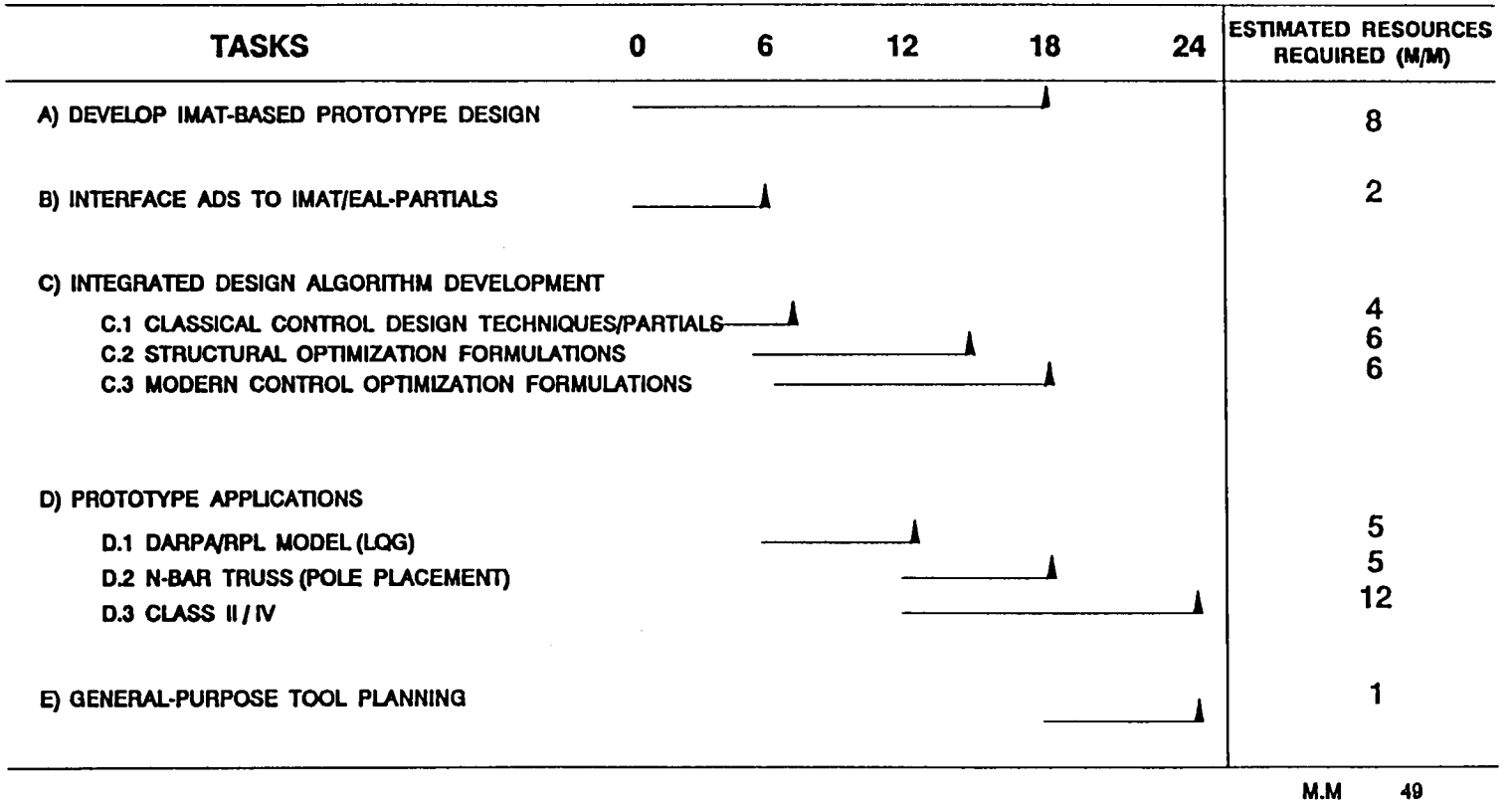

Figure 25. Proposed Program Plan for Integrated Design

References

Adamian, A. and Gibson, J.S., "Integrated Control/Structure Design and Robustness", SAE paper 861821, Aerospace Technology Conference and Exposition, Long Beach, CA. October 13-16, 1986.

Arora, J.S., Thanedar, P.B., and Tseng, C.H., "User's Manual for Program IDESIGN", Technical Report No. ODL 85.10, University of Iowa, Iowa City, May 1985.

Becus, G.A., Lui, C.Y., Venkayya, V.B. and Tischler, V.A., "Simultaneous Structural and Control Optimization via Linear Quadratic Regulator Eigenstructure Assignment", NASA CP-2488, Oct. 1987, pp. 225-232.

Bellagamba, L. and Yang, T.Y., "Minimum-Mass Truss Structures with Constraints on Fundamental Natural Frequency", AIAA Journal, vol. 19, no. 11, Nov. 1981, pp. 1452-1458.

Belvin, W.K. and Park, K.C., "Structural Tailoring and Feedback Control Synthesis: An Interdisciplinary Approach", AIAA 88-2206, pp. 1-8.

Belvin, W.K. and Park, K.C., "On the State Estimation of Structures with Second Order Observers", AIAA 89-1241, AIAA/ASME/ASCE/AHS 30th Structures, Structural Dynamics, and Materials Conference, Mobile, Alabama, April 3-5, 1989.

Belvin, W.K. and Park, K.C., "Computational Architecture for Integrated Controls and Structures Design", Third Annual NASA/DOD CSI Conference, San Diego, CA, January 29-February 2, 1989.

Bodden, D.S. and Junkins, J.L., "Eigenvalue Optimization Algorithms for Structure/Controller Design Iterations", J. Guidance and Control, Vol. 8, 1985, pp. 687-706.

Bogomolny, A., and Hou, J.W., "Shape Optimization Approach to Numerical Solution of the Obstacle Problem", Appl. Math. Optim. 12:45-72(1984).

Boyd, S.P., Balakrishnan, V., Barrat, C.H., Khraishi, N.M., Li, X., Meyer, D.G., and Norman, S.A., "A New CAD Method and Associated Architectures for Linear Controllers", IEEE Transactions on Automatic Control, Vol. 33, No. 3, Mar 1988, pp. 268-283.

Canfield, R.A., Grandhi, R.V. and Venkayya, V.B., "Optimum Design of Large Structures with Multiple Constraints", Proceedings of the 27th Structures, Structures Dynamics, and Materials Conf., San Antonio, TX, May 19-21, 1986, pp. 398-408.

Choi, K.K., Haug, E.J., and Seong, H.G., "An Iterative Method for Finite Dimensional Structural Optimization Problems with Repeated Eigenvalues", International Journal for Numerical Methods in Engineering, Vol. 19, pp. 93-112, 1983.

Chun, H.M., "Large-Angle Slewing Maneuvers for Flexible Spacecraft," Ph.D. dissertation, Department of Aeronautics and Astronautics, Massachusetts Institute of Technology, 1986.

Chun, H.M., Turner, J.D., and Juang, J.N., "Frequency-Shaped Large-Angle Maneuvers, " Paper AIAA-87-0174, presented at the AIAA 25th Aerospace Sciences Meeting, Reno, Nevada, January 12-15, 1987.

Chun, H.M., and Turner, J.D., "Large-Angle Slewing Maneuvers for Flexible Spacecraft, "NASA Contractor Report 4123, Contract NAS1-18098, February 1988.

Chun, H.M., Turner, J. D., and Frisch, H.P., "Experimental Validation of Order(n) DISCOS," Paper AAS 89-457, AAS/AIAA Astrodynamics Specialist Conference, August 1989.

Cooper, P.A., Young, J.W., and Sutter, T.R., "Multidisciplinary Analysis of Actively Controlled Large Flexible Spacecraft", First NASA/DOD CSI Technology Conference, Nov. 18-21, 1986, Norfolk, VA.

Crane, R.L., Hillstrom, K.E., and Minkoff, M., "Solution of the General Nonlinear Programming Problem with Subroutine VMCOM", Argonne National Laboratory, ANL-80-64, 1980.

Cronin, D.L., "Perturbation Approach for Determining Eigenvalues and Eigenvectors for Nonproportionally Damped Systems", Proceedings for the 6th International Modal Analysis Conference, Kissimmee, Fl., February 1-4, 1988, pp. 23-29.

Desoer, C.A. and Gustafson, C.L., "Algebraic Theory of Linear Multivariable Feedback Systems", IEEE Trans. Automat. Contr., Vol, AC-29, pp. 909-917, Oct. 1984.

Doyle, J.C., "Analysis of Feedback Systems with Structured Uncertainties", IEEE Proc, Vol. 129, Nov., 1982.

Doyle, J.C., and Stein, G., "Multivariable Feedback Design: Concepts for a Classical/Modern Synthesis", IEEE Trans. Automat. Contr., Vol, AC-26, pp. 4-16, Feb. 1981.

Fanson, J.L., Blackwood, G.H., and Chu, C-C., "Active Member Control of Precision Structures," AIAA Paper 89-1329, 30th AIAA/ASME/ASCE/AHS Structures, Structural Dynamics and Material Conference, Mobil, Alabama, 1989.

Fleury, C. and Schmit, L.A., "Dual Methods and Approximation Concepts in Structural Synthesis", NASA CR-3226, Dec. 1989.

Foss, K.A., "Coordinates which Uncouple the Equations of Motion of Damped Linear Dynamic Systems", Trans. ASME J. Applied Mech., 25, pp. 361-364, 1958.

Fox, R.L. and Kapoor, M.D., "Rates of Change of Eigenvalues and Eigenvectors", AIAA Journal, vol. 6, Dec. 1968, pp. 2426-2429.

Francis, B.A. and Zames, G., "On H-inf Optimal Sensitivity Theory for SISO Feedback Systems", IEEE Trans. Automat. Contr, Vol, AC-29, pp. 9-16, Jan. 1984.

Fraser, D.C., "Aircraft Control Systems--A Projection to the Year 2000", IEEE Control Systems Magazine, Feb. 1985, pp. 11-13.

Garibotti, J.G., "Requirements and Issues for the Control of Flexible Space Structures", Proceedings of the 25th AIAA/ASME/ASCE/AHS Structures Dynamics and Materials Conference, Washington, DC, 1984, pp. 338-347.

Gill, P.E., Murray, W., and Wright, M., Practical Optimization, New York: Academic, 1981.

Gill, P.E., Murray, W., Saunders, M.A., and Wright, M.H., "User's Guide for NPSOL (Version 4.0): A Fortran package for nonlinear programming", Dept. Operat. Res., Stanford Univ., Stanford, CA, Tech. Rep. SOL 89-2, Jan. 1986.

Gill, P.E., Hammarling, S.J., Murray, W., Saunders, M.A., and Wright, M.H., "User's Guide for LSSOL (Version 1.0): A Fortran package for constrained least-squares and convex quadratic programming", Dept. Operat. Res., Stanford Univ., Stanford, CA., Tech. Rep. SOL 86-1, Jan. 1986.

Goldfarb, D., "Extensions of Davidson's Variable Metric Method to Maximization Under Linear Inequality and Equality Constraints", SIAM Journal of Applied Mathematics, vol. 17, 1969, pp. 739-764.

Grandhi, R.V., Thareja, R., and Haftka, R.T., 'NEWSUMT-A: A General Purpose Program for Constrained Optimization Using Constraint Approximations", ASME J. Mechanism, Transmission, and Automation in Design, Vol. 107, March 1985, pp. 94-99.

Grandhi, R.V. and Venkayya, V.B., "Structural Optimization with Frequency Constraints", Proceedings of the AIAA/ASME/ASCE/AHS 28th Structures, Structural Dynamics, and Material Conference, 1987, pp. 322-332.

Gupta, N.K., "Frequency-Shaped Cost Functionals: Extension of Linear-Quadratic-Gaussian Design Methods," Journal of Guidance and Control, Vol. 3, No. 6, November-December 1989, pp. 529-535.

Gustafson, C.L., Aswani, M., Doran, A.L. and Tseng, G.T., "ISAAC (Integrated Structural Analysis and Control) Via Continuum Modeling and Distributed Frequency Domain Design Techniques", Proceedings of the Workshop on Identification and Control of Flexible Space Structures, Jet Propulsion Laboratory, Pasadena, CA., JPL 85-29, April 1985, pp. 2878-310.

Haftka, R.T., Martinovic, Z.N., Hallauer, W.L. and Schamel, G., "Sensitivity of Optimized Control Systems to Minor Structural Modifications", Proceedings of the 26th AIAA/ASME/ASCE/AHS Structures, Structural Dynamics and Materials Conference, Washington, DC, April, 1985, pp. 642-650.

Haftka, R.T., Martinovic, Z. and Hallauer, Jr., W.L., "Enhanced Vibration Controllability by Minor Structural Modifications", AIAA Journal, Vol. 23, No. 8, August 1985, pp. 1260-1266.

Hale, A.L., Lisowski, R.J. and Dahl, W.E., "Optimal Simultaneous Structural and Control Design of Maneuvering Flexible Spacecraft", J. Guidance and Control, Vol. 8, No. 1, Jan-Feb 1985, pp. 86-93.

Hale, A.L., "Integrated Structural/Control Synthesis Via Set - Theoretic Methods", AIAA/ASME/ASCE/AHS 26th SEM Conference, Orlando, FL, 85-0806-cp, April, 1985.

Hanks, B.R. and Skelton, R.E., "Designing Structures for Reduced Response by Modern Control Theory", AIAA Paper 83-0815, May 1983.

Haug and B. Rousselet, "Design Sensitivity Analysis in Structural Mechanics, Part I: Static Response Variations", J. Struct. Mech., Vol. 8, no. 1, pp. 17-41, 1980.

Haug, E.J. and Rousselet, Design Sensitivity Analysis in Structural Mechanics, Part II: Eigenvalue Variations", J. Struct. Mech., Vol. 8, no. 2, pp. 161-186, 1980.

Heylen, W., "Model Optimization with Measured Modal Data by Mass and Stiffness Matrix Changes", Proc. of the 4th Int. Modal Analysis Conf., pp. 94-100, Los Angeles, CA, 1986.

Hou, J.W. and Twu, S.L., "Optimum Design for Internal Strain-Gage Balances: An Example of Three-Dimensional Shape Optimization", Transaction of the ASME, Journal of Mechanisms, Transmissions, and Automation in Design, 86-DET-27, pp. 1-6.

Juang, J.N. Lim, K.B., and Junkins, J.L., "Robust Eigensystem Assignment for Flexible Structures", AIAA 87-2252, pp. 117-123.

Junkins, J.L., Bodden, D.S. and Turner, J.D., "A Unified Approach to Structure and Control System Design Iterations", Fourth Intl. Conf. on Applied Numerical Modeling, Tainan, Taiwan, Dec., 1984.

Junkins, J.L. and Rew, D.W., "A Simultaneous Structure/Controller Design Iteration Method", American Controls Conference, Boston, MA, June 1985.

Kamat, M.P., Venkayya, V.B. and Khot, N.S., "Optimization with Frequency Constraints Limitations", Journal of Sound and Vibration, 91(1), 1983, pp. 147-154.

Khot, N.S., "Optimization of Structures with Multiple Frequency Constraints", Computers & Structures, 20(5), 1985, pp. 869-876.

Ketner, G.L., "Survey of Historical Incidences with Controls-Structures Interaction and Recommended Technology Improvements Needed to Put Hardware in Space", Battelle Pacific Northwest Laboratory Report no. PNL-6846, UC-222.

Khan, M.R., Thornton, W.A. and Willmert, K.D., "Optimization of Structures with Multiple Design Variables per Member", AIAA Journal, Vol. 20, Sept. 1982, pp. 1282-1283.

Khot, N.S., Grandhi, R.V. and Venkayya, V.B., "Structural and Control Optimization of Space Structures", AIAA/ASME/ASCE/AHS 28th Structures, Structural Dynamics and Materials Conference, April 6-8, 1987, vol. 2b, paper no. 87-0939, pp. 850-860.

Khot, N.S., "An Integrated Approach to the Minimum Weight and Optimum Control Design of Space Structures", Large Space Structures: Dynamics and Control, Springer-Verlag Berlin Heidelberg, 1988, pp. 355-363.

Khot, N.S., Oz. H., Grandhi, R.V., Eastep, R.E. and Venkayya, V.B., "Optimal Structural Design with Control Gain Norm Constraint", AIAA 25th Aerospace Sciences Meeting, Reno, NV, 1987.

Khot, N.S., Eastep, F.E. and Venkayya, V.B., "Optimal Structural Modifications to Enhance the Optimal Active Vibration Control of Large Flexible Structures", AIAA Journal, Vol. 24, No. 8 1986, pp. 1368-1374.

Kyong, L.B. and Junkins, J.L., "Robustness Optimization of Structural and Controller Parameters," J. of Guid. and Control, July-Aug 88.

Lim, K.B. and Junkins, J.L., "Minimum Sensitivity Eigenvalue Placement via Sequential Linear Programming", Proceedings of the Mountain Lake Dynamics and Control Institute, ed. by J.L. Junkins, Mountain Lake, Va, June 9-11, 1985.

Lim, K.B. and Junkins, J.L., "Optimal Redesign of Dynamic Structures via Sequential Linear Programming", Fourth International Modal Analysis Conference, Los Angeles, CA, Feb. 3-6, 1986.

Longman, R. and Alfriend, K.T., "Energy Optimal Degree of Controllability and Observability for Regulator and Maneuver Problems," The Journal of the Astronautical Sciences, Vol. 38, No. 1, pp. 87-103, January-March 1990.

Lust, R.V. and Schmit, L.A., Alternative Approximation Concepts for Space Frame Synthesis", AIAA Journal, vol. 24, Oct. 1986, pp. 1676-1684.

Lust, R.V. and Schmit, L.A., "Control Augmented Structural Synthesis", AIAA/ASME/ASCE/AHS 27th SDM Conference, San Antonio, TX, 86-1014-CP, 1986.

Lust, R.V. and Schmit, L.A., "Control-Augmented Structural Synthesis", AIAA Journal, vol. 26, no. 1, January 1988, pp. 86-95.

Ly, U.-L, Bryson, A.E. and Cannon, R.H., "Design of Low-Order Compensators Using Parameter Optimization", Applications of Nonlinear Programming to Optimization and Control, IFAC, 1983.

Manning, R.A. and Schmit, L.A., "Control Augmented Structural Synthesis with Transient Response Constraints", 87-0749, 87-AIAA, pp. 194-204.

Messac, A., Turner, J. and Soosaar, K., "An Integrated Control and Minimum Mass Structural Optimization Algorithm for Large Space Structures", Jet Propulsion Workshop on Identification and Control of Flexible Space Structures, San Diego, CA., June 1984.

Miller, D.F. and Shim, J., "Gradient-Based Combined Structural and Control Optimization", J. Guidance, 10(3), May-June 1987, pp. 291-298.

Miller, D.F. and Shim, J., "Combined Structural and Control Optimization for Flexible Systems Using Gradient Based Searches", AIAA 24th Aerospace Sciences Meeting, Reno, NV, 1986.

Miller, D.F., Venkayya, V.B., Oz, R.V., Grandhi, R.V. and Eastep, F.E., "Optimal Structural Design with Control Gain Norm Constraint", AIAA-87-0019, AIAA 25th Aerospace Sciences Meeting, Reno, Nevada, Jan. 12-15, 1987.

Miller, D.F. and Shim, J., "Combined Structural and Control Optimization for Flexible Systems Using Gradient Based Searches", AIAA-86-0178, AIAA 24th Aerospace Sciences Meeting, January 6-9, 1986, Reno, Nevada.

Mills-Curran, W.C., Lust, R.V. and Schmit, L.A., "Approximation Methods for Space Frame Synthesis", AIAA Journal, Vol. 21, Nov. 1983, pp. 1571-1580.

Newsom, J.R. and Muknopadhyay, "A Multiloop Robust Controller Design Study Using Singular Value Gradients", Journal of Guidance and Control, Vol. 8, no. 4, July-August 1985, pp. 514-519.

Onoda, J. and Haftka, R.T., "Simultaneous Structure/Control Optimization of Large Flexible Spacecraft", AIAA 87-0823, pp. 501-507.

Onoda, J. and Haftka, R.T., "An Approach to Structure/Control Simultaneous Optimization for Large Flexible Spacecraft", AIAA Journal, vol. 25, no. 8, Aug. 1987, pp. 1133-1138.

Palacios-Gomez, F., "The Solution of Nonlinear Optimization Problems Using Successive Linear Programming", PhD. Dissertation, The University of Texas, Austin, TX, 1980.

Park, K.C. and Belvin, W.K., "Stability and Implementation of Partitioned CSI Solution Procedures", AIAA 89-1238, AIAA/ASME/ASCE/AHS 30th Structures, Structural Dynamics, and Materials Conference, Mobile, Alabama, April 3-5, 1989.

Pedersen, P., "Design with Several Eigenvalue Constraints by Finite Elements and Linear Programming", J. Struct. Mech., 10(3), 243-271, 1982.

Photon Research Associates, "Control-Structure-Interaction (CSI) Technologies and Trends for Future NASA Missions: NASA CR187471, 1990.

Plaut, R.H. and Huseyin, K., "Derivatives of Eigenvalues and Eigenvectors in Non-Self-Adjoint Systems", AIAA Journal, Vol. 11, No. 2, pp. 250-251, Feb. 1973.

Polak, E., Siegel, P., Wuu, T., Nye, W.T. and Mayne, D.Q., "DELIGHT.MIMO: An Interactive, Optimization-Based Multivariable Control System Design Package", Computer-Aided Control System Engineering, M. Jamshidi and C. J. Herget, EDS. Amsterdam, The Netherlands: North-Holland, 1985.

Prasad, B., "Novel Concepts for Constraint Treatments and Approximations in Efficient Structural Synthesis", AIAA Journal, vol. 22, July 1984, pp. 957-966.

Rubin, C.P., "Minimum Weight Design of Complex Structures Subject to a Frequency Constraint", AIAA Journal, vol. 8, May 1970, pp. 923-927.

Rudisill, S., "Derivatives of Eigenvalues and Eigenvectors for a General Matrix", AIAA Journal, Vol. 12, No. 7, pp. 721-722, 1974.

Safonov, M.G., "Optimal Diagonal Scaling for Infinity-Norm Optimization", Syst. Contr. Lett., vol. 7, pp. 257-260, 1986.

Salama, M., Hamidi, M. and Demsetz, L., "Optimization of Controlled Structures", Jet Propulsion Workshop on Identification and Control of Flexible Space Structures, San Diego, CA, 1984.

Shiau, T.N. and Chang, S.J., "Minimum Weight Design of Rotating Pretwisted Blades with Dynamic Behavior Constraints", AIAA Paper no. 88-2267, pp. 441-448.

Shin, Y.S., Plaut, R.H. and Haftka, R.T., "Simultaneous Analysis and Design for Eigenvalue Maximization", AIAA 87-0788, pp. 334-342.

Sobieski, J., "A Linear Decomposition Method for Large Optimization Problems - Bluepoint for Development", NASA TM-83248, February 1982.

Sobieski, J., "Multidisciplinary Systems Optimization by Linear Decomposition", Proceedings of the Symposium on Recent Experiences in Multidisciplinary Analysis and Optimization, NASA Conference Publication 2327, Part 1, Ed. Sobieski, J., pp. 343-366, 1984.

Thareja, R. and Haftka, R.T., "Numerical Difficulties Associated with Using Equality Constraints to Achieve Multi-Level Decomposition in Structural Optimization", AIAA 86-0854, pp. 21-28.

Tseng, C.H. and Arora, J.S., "Optimum Design of Systems for Dynamics and Controls Using Sequential Quadratic Programming", AIAA 88-2303, pp. 739-745.

Tseng, C.H. and Arora, J.S., "On Implementation of Computational Algorithms for Optimal Design: "Preliminary Investigation," International Journal for Numerical Methods in Engineering, vol. 26, 1365-1366 (1988).

Turner, M.J., "Design of Minimum Mass Structures with Specified Natural Frequencies", AIAA Journal, vol. 5, no. 3, March 1967, pp. 406-412.

Vanderplaats, G.N., "CONMIN--A Fortran Program for Constrained Function Minimization", NASA TM X-62282, Aug. 1973.

Vanderplaats, G.N., "ADS-A FORTRAN Program for Automated Design Synthesis-Version 1.00", NASA CR-172460, Oct. 1984.

Vanderplaats, G.N., "Numerical Optimization Techniques for Engineering Design with Applications, McGraw-Hill Book Company, 1984.

Vanderplaats, G.N., "An Efficient Feasible Direction Algorithm for Design Synthesis", AIAA Journal, 22(11), 1984, pp. 1633-1640.

Venkayya, V.B. and Tischler, V.A., "ANALYZE: Analysis of Aerospace Structures with Membrane Elements", AFFDL-TR-78-170, 1978.

Venkayya, V.B. and Tischler, V.A., "OPTSTAT: A Computer Program for the Optimal Design of Structures Subjected to Static Loads", AFFDL-TM-FBR-79-67, June 1979.

Viswanathan, C.N., Longman, R.W., and Likins, P.W., "A Degree of Controllability Definition: Fundamental Concepts and Application to Modal Systems," Journal of Guidance, Control and Dynamics, pp. 222-230, March-April, 1984.

Walsh, J.L., "Optimization Procedure to Control the Coupling of Vibration Modes in Flexible Space Structures", AIAA 1987, 87-0826, pp. 525-536.

Wang, B.P., "Synthesis of Structures with Multiple Frequency Constraints", Proceedings of the 27th Structures, Structural Dynamics, and Materials conf., San Antonio, TX, May 19-21, 1986, pp. 394-397.

Woo, T.H., "Space Frame Optimization Subject to Frequency Constraints", AIAA Journal, vol. 25, no. 10, Oct. 1987, pp. 1396-1404.

Yoshida, N. and Vanderplaats, G.N., "Structural Optimization Using Beam Elements", AIAA/ASME/ASCE/AHS 26th Structures, Structural Dynamics and Materials Conference, Orlando, FL., April 1985.

Zeischsha, H., Leuridan, J., Storrer, O., and Vandeurzen, H., "Calculation of Modal Parameter Sensitivities Based on a Finite Element Proportionality Assumption", Proceedings of 6th International Modal Analysis Conf., February 1-4, 1988, Kissimmee, Florida, pp. 1082-1087.

End of Document